The overpressure driven seismic velocity response. The review of standard models and methods for extraction in the context of basin modelling approach to overpressure prediction

A.G. Madatov
Higher Mathematics Chair of the Polytechnical Faculty, MSTU

Abstract. The seismic velocity analysis in reflection wave method has been traditionally applied for the pre-drill prediction of overpressured subsurface formations since the early 1960s. The location of the first successful implementations was the Gulf of Mexico, where thick Pleistocene-Miocene sediments are represented by clastic rock, which are poorly consolidated at the upper part of the section and are often overpressured from the very top. Despite of long implementation history this application of the seismic method remains to be questionable in other sedimentary basins especially those where exploration targets are associated with Mesozoic and older interval of the sections. Here velocity based prediction of over-hydrostatic pressured formations becomes hazardous and uncertain operation. The main reasons of these facts are: low sensitivity of the velocity derived overpressure response inherent for consolidated clastic and carbonate rocks; essentially 1-D mechanical compaction non-adequate model of multi-mechanism overpressure phenomenon; natural limitation in seismic wave spatial resolution; non-purposely oriented seismic data processing, where compressional/shear wave velocity is not treatable as a rock property. The majority of published about this topic reviews were focused on last two problems trying to find the best solution on the way of purpose-built processing strategy and perfecting seismic data inversion approaches. This paper reviews theoretical velocity models applicable for description of a target phenomenon in connection with results of ultra-sonic lab measurements and empirical relationships established for seismic frequency band. The error free (direct) overpressure response potentially detectable from velocity data is analysed on this ground for different depth intervals of the section. The sand, shale and carbonate lithologies are distinguished. The relevant normalised anomaly is estimating for speculative and real case examples. The combining of basin scale models of deposystem evolution with full waveform inversion approach is suggested as a proper way for developing the relevant multi-disciplinary strategy of overpressure prediction.

1. Introduction

The prevention of drilling mud losses or kicks, the drilling risk assessment in connection with expected formation pressure, the casing design and so on are typical industry problems associated with prediction and estimation of pore pressure before and during exploration well drilling (*Bell*, 1994; *Huffman*, 2002).

Up to now seismic velocities in their different modifications remain major and often the only input for pre-drill (before starting of exploration well drill operations) prediction. This is especially true for virgin areas or/and frontier depth intervals[1] within the explored areas. In both cases offset wells with attached drilling information appear to be not available.

An extraction of the target overpressure signal from seismic velocity input is based on theoretically predicted and practically proven facts that excess hydrostatic pressure (overpressure anomaly) can somehow be recorded in seismic data and is extractable and interpretable from the relevant seismic velocity information. Roughly, the overpressure phenomenon affects the elastic properties of sedimentary rocks in the way which produces the negative departure of seismic velocity from values normally expected in agreement with positive velocity trend observed along coinciding directions: depth-temperature increase and rock consolidation (*Pennebaker*, 1968; *Reynolds*, 1970; *Gardner et al.*, 1974; *Keyser et al*., 1991; *Dutta, Ray*, 1996). In this paper let us call this target phenomenon – *Overpressure Driven Velocity Response* (ODVR).

Note, that the overpressure response potentially observable and extractable from amplitude characteristics of seismic wave field such as frequency depended attenuation and quality factor cannot be considered so far as a traditional input in the context of overpressure prediction. Their applicability to these purposes remains to be proven on practice despite the optimism announced from researchers' side (*Kuster, Toksoz*, 1974; *Carcione, Helle*, 2002). Whether or not this optimism is justified will show time and drilling experience. Our own experience in particular shows that the target overpressure signal is to a considerable extent disguised in a seismic wave field dynamics and its extraction constitutes even more challenge task for processing and interpretation than it is for cinematically controlled velocity response (*Madatov et al*., 1991; 1996a). The reviewing and verifications of these prediction approaches are far beyond the scope of our current discussion. Still we believe that the majority of

[1] Deeper then ever has been drilled before.

general statements and conclusions made in the given paper remains to be valid for any other seismically driven overpressure indicators in context of generic overpressure prediction strategy.

The pre-drill strategy of overpressure prediction based on the ODVR phenomenon always implied processing and *interpretation* phases which are implicitly carrying connotations of *uncertainty.* The history of its implementation was started from the first experiences in the Gulf of Mexico onshore (*Pennebaker*, 1968) and the Caspian Sea offshore (*Dobrynin, Serebryakov*, 1978). By now the practical experience indicates more and more restrained estimations of the finally achievable accuracy of this prediction and its applicability for deeper HC targets (*Al-Ghalabi*, 1994; *Khazanehdari et al.*, 1998; *Campbell et al.*, 2000; *Dutta*, 2002a). The universally recognised expert N. Dutta in his recent review (*Dutta*, 2002b) stressed that "methods based on seismic information have validity naturally restricted by vertical and lateral resolution of seismic reflection method and are not reliable unless sensitive to overpressure parameter velocity is conditioned for purposes by using model oriented processing approaches". If to take into account that the majority of well proven successive applications of the ODVR based on pre-drill prediction come from Tertiary clastic sections with geologically short and continuous burial history, the prospects of standard strategy for older and less homogeneous sections turn out to be not very clear and promising.

The general conclusion about increasing of drilling risk challenge (*Huffman*, 2002) with the depth and age of exploration targets is as much generally correct as not specific for specific regions.

Most of the published discussions around these problems were focused on seismic input improvements required for prediction purposes through all the work-flow stages from data acquisition up to velocity aimed processing and analysis (*Mathew, Kelly*, 1967; *Reynolds*, 1970; *Urupov, Levin*, 1985; *Bilgeri, Ademeno*, 1982; *Keyser et al*., 1991; *Bangs et al*., 1996; *Traugott*, 1997; *Sayers et al*., 2002). As to the conversion of rock velocity anomaly to overpressure anomaly it was considered to be unique and stable operation based on simple bijective Terzaghi' one-axial stress model (*Terzaghi, Peck*, 1948). The closer investigations (*Waples, Kamata*, 1993; *Schneider et al*., 1994; *Swarbrick, Osborne*, 1996), however, reveal that validity of this mechanical compaction model is rather restricted by clay-shale lithology and sediment rock consolidation depth gape with no significant erosion and diagenetic processes during burial history.

The attempts to extend this mechanical model to more general case led to creation hybrid type of the Earth models combining elements of basing scale geo-fluid dynamics with principles of 1-D rock mechanic (*Bowers*, 1995; *Seberyakov et al*., 1995). Still the departure of rock velocity from the trend line/range of values associated with normally stressed porous rock remains mainly sensitive to overpressure seismically driven response.

How adequate is such approach to the new reality, which dictates involving new, more sophisticated Earth model to account for other overpressuring mechanisms apart from compaction disequilibrium? What are the weakest points in seismically driven overpressure prediction in context of deepening of new potential exploration targets? How can drilling surprises be avoided in advance by taking into account inherent restriction of the considered method in resolution and validity in more complex geological conditions? Are any more generally applicable Earth models and the relevant methods more viable and less risky in new harder conditions to assess quality of pre-drill overpressure prediction and control it during drilling? If so, where are the links between new and old well proven models/methods and how can they be combined?

These questions have given the main impetus for the given paper and have formed its style and architecture.

2. Short review of the forward poroelasticity models describing seismic velocities

When discussing detection of such a natural phenomenon, like pore pressure in situ, it is important to correlate in mind the micro scale of the phenomenon and macro scale of surface seismic data acquisition. The target elastic property – velocity of seismic wave propagation – delivers some micro scale information in a rather filtered form. In general, a value of seismic velocity cumulatively combines effects of representative rock volume elastic property, seismic wave property, source-receiving system property and seismic processing characteristics (including interpretation model, noise & signal definitions, parameters of computation, etc.).

In context of pore pressure detection from seismic velocity it is important to specify the appropriate class of elastic media models, where this micro scale property can be made available as a representative rock property and be conditioned for overpressure prediction.

Below in this paper we will use term *rock seismic velocity* or just *seismic velocity* to recognise this elastic characteristic of real medium as a rock property aimed for investigation and analysis of some target phenomena in contrast to seismic wave field velocity as an effective parameter associated with the relevant data processing (*Dix*, 1955; *Urupov, Levin*, 1985). The target phenomenon in our paper is overpressure. Still the seismic velocity delivers some information about lithology changes (*Averbukch*, 1982), fluid phase content changes (*Gardner et al*., 1974), shale anisotropy (*Vernik*, 1994), etc. Thus, discussing any of such phenomena manifestations via seismic velocity we will imply the relatively conditioned rock property.

As it is generally agreed (*Domenico*, 1976; *Gregory*, 1976; *Averbukch*, 1982; *White*, 1983; etc), "homogeneity" is not an absolute characteristic of matter, but is a term applicable to properties averaged over

some suitable volume. "Even the most uniform material is made up of atoms, so its properties are grossly non-uniform when viewed on a small enough scale. Material made of obvious structural elements may be highly uniform when viewed on a large scale. If choice of scale were entirely arbitrary, the term "homogeneity" would not be particularly useful. The context always provides some reference length to serve as a scale of measurement, which for elastic-wave propagation is a wavelength" (*White*, 1983).

According to definition a medium is homogeneous if its properties are the same when averaged throughout any elementary volume in the medium, an elementary volume being defined as the largest volume whose linear dimensions are small compared with the shortest wavelength of importance. This determination is applicable for seismic and acoustic wave propagation in heterogeneous media. Laminated solids, granular media, fractured rocks and liquid suspensions are discussed below, to show how elastic constants and wave speeds can be derived for such materials.

The average length of seismic wavelet radiated at 30-60 Hz band and reflected then from shallow (first hundred of meters) and deep (first thousands of meters) subsurface horizons in sedimentary basins is typically ranging at about $K\times10^1$ – $M\times10^2$ m depending on the type of elastic deformation (compression or shear) and the rock type. The scale of averaging for ultrasonic waves is respectively detailer on 3-4 orders.

As we are focusing on seismic band of waves, it is important to stress that elastic properties of media even in the homogeneous case imply some natural averaging (low frequency band pass filtering) over different materials and hence are available for surface measurements in the cumulative form. For example, the laminated solid with thickness of each individual horizontal layer not higher then 10 cm will be visible as a transversely isotropic homogeneous medium or as a thin layered stack at the seismic or acoustic bands, respectively. Strictly speaking, recovering of in situ elastic modulus for pure solid material from seismic experiment in the form comparable with lab experiments is not possible. Between pure solid properties and in situ rock properties we always have some underlying local level model of spatial sorting and regulation like laminated solids, granular media, porous media, fractured rocks, liquid suspensions, etc. Each of such models implies specific technique for upscaling. For example, (*Backus*, 1962) has derived expression for weighted averaging of elastic constants for the horizontally laminated solid model.

Still, any of these models must be formed from some ideally purified prototype of a homogeneous isotropic medium. There are two cases distinguished for such prototype models: continuous elastic case and poro-elastic case, where the second one could be derived from the first one. Now we will consider both of them briefly.

2.1. A purified elastic model

In general, the elastic behaviour of a medium is defined by the equation

$$\sigma_{ij} = C_{ijkl}\varepsilon_{kl}, \tag{1}$$

where σ_{ij} and ε_{kl} are the stress and strain components and C_{ijkl} denotes the tensor of the stiffness constants. In the most general case, C_{ijkl} contains 21 independent constants, but according to the symmetry properties of the medium the number of independent components can be substantially reduced. For example, the trigonal quartz crystal has six and the hexagonal ice crystal – five independent parameters (*Keller et al*., 1999).

In the purified case of a homogeneous isotropic medium, the stress-strain relationship is represented by two independent elastic constants – modulus of elasticity or Young's modulus. The main measurable while seismic exploration elastic property of a subsurface medium are velocities of two elastic body waves. They can be represented via the pair of the shear (G) and bulk (K) modulus or via the Young's module E and Poisson's ratio γ as the following:

$$\begin{cases} V^H_p = [(K + 4G/3)/\rho]^{1/2} = [E(1-\rho)/\rho(1+\gamma)(1-2\gamma)]^{1/2}; & (2) \\ V^H_s = (G/\rho)^{1/2} = [E(1-\rho)/\rho\,(1+\gamma)^2]^{1/2}, & (2^*) \end{cases}$$

where V^H_p and V^H_s are the longitudinal compression and transverse shear waves propagation velocities, respectively, and the upper index H indicates relation to the homogeneous isotropic case; ρ is the density of the medium. The (V_p/V_s) ratio is an important seismic diagnostic parameter, since it removes influence of rock density effect.

However, it is important to stress that the purified homogeneous isotropic model of media can only be applied when the impact of micro-scale properties such as grain to grain contact, type of in situ grain packing, pore space fabric and so on the elastic modulus of solid matrix can be ignored. Evidently, that this speculative class of the velocity models is not workable for investigation of real properties of a natural rock-fluid system. It is especially true, when the target is pore fluid phenomenon.

2.2. Low frequency Gassmann's model

At low (seismic) frequencies, the effects of the presence of pore fluid on the velocities of longitudinal compressional (P) and transverse shear (S) waves can be described by Gassmann's (1951) theory (*Gassmann*, 1951; *White*, 1983; *Nur, Wang*, 1992). The relevant fluid-saturated porous rock model according to this theory reveals velocity vs. elastic modulus relationship in the following modified in comparison with (2-2*) form:

$$\begin{cases} V^G_p = [(K_b + 4G/3 + \nu^2 M)/\rho_b]^{1/2}; & (3) \\ V^G_s = (G/\rho_b)^{1/2}, & (3^*) \end{cases}$$

where the Biot cross coefficient M is given by $1/M = \phi/K_f + (\lambda - \phi)/K_s$ and $\nu = 1 - K_b/K_s$ in which K_b denotes the bulk modulus of the dry porous rock, G denotes the shear modulus of the dry porous rock. K_s denotes the bulk modulus of the solid rock matrix material, K_f – the bulk modulus of the fluid saturating the porous rock, ϕ – the porosity of the rock, $\rho_B = \rho_s(1 - \phi) + \rho_f\phi$ denotes the bulk density of the porous rock, ρ_f – the density of the fluid saturating the pore space and ρ_s – the density of the solid matrix material. The index "^{G}" indicates the Gassmann's model.

Basically, there are at least five important assumptions underlying of Gassmann's (1951) theory. They are the following:

1. The porous rock is homogeneous and isotropic.
2. The pores are interconnected (there are no isolated pores).
3. The pore fluid is frictionless (low-viscosity fluid).
4. Relative motion between fluid and solid during the passage of an elastic wave is negligible (low frequencies only).
5. The pore fluid does not interact with the solid matrix material (the matrix elastic moduli are unaffected by fluid saturation).

R. Brown and J. Korringa (1975) found more general form of Gassmann's model, which accounts for non-homogeneous and isotropic solid rock frame (conglomerates) and porous fluid at given differential pressure, i.e. which extends the relevant poro-elasticity equation in case that ignores assumption (1). According to them the Biot cross coefficient is becoming the function of differential pore pressure (P_Δ), which is defined as a difference between confining pressure and fluid pressure. Thus, the Biot cross coefficient was given in a new model by:

$$1/M(P_\Delta) = \phi/K_f + \lambda/K_s + \phi/K_p(P_\Delta), \tag{4}$$

where K_p is an additional elastic parameter associated with the pore volume changes when the fluid pressure and confining pressure are increasing keeping differential pressure fixed. Later *J. Berryman and G. Milton* (1991) extended model (4) on more general case, when differential pressure and pore fluid pressure are changing independently in a linear composite at every given confining pressure. This extension requires one additional parameter $C_p(P_\Delta)$ in order to describe the current pressure combination and especial averaging technique.

Recently, one more generalisation of Gassmann's velocity model came from the Stanford University research group. A. Nur and J. Dvorkin have showed that empirical relations generally fail to predict velocity-porosity relations outside the range of values for which they are estimated. In order to improve this situation they proposed to distinguish between two levels of porosity for in situ sedimentary rock: below and above a *Critical porosity* – ϕ_c. They have introduced the *Critical porosity* as a fundamental property of the porous system and extended elastic module determination to the following form (*Nur, Dvorkin*, 1998):

$$\begin{cases} M_V = (1 - \phi)\, M_S + \phi\, M_f & \text{at } \phi < \phi_c; \\ M^{-1}_R = (1 - \phi)\, M^{-1}_S + \phi\, M^{-1}_f & \text{at } \phi \geq \phi_c, \end{cases} \tag{5}$$

where M_S and M_f are the moduli of the solid and the pore filling materials, respectively, and ϕ is the porosity. Here the lower indices indicate Voigt (M_V) and Reuss (M_R) averaging valid for grains' well contacted and poor contacted (suspension of grains) cases, respectively.

Roughly, the Critical Porosity can be defined as a porosity at which the in situ load on porous rock transforms from fluid to solid load-bearing. Consequently, this characteristic is a property of the porous system, not just of one of its component. It significantly varies with lithology variation. For example, ϕ_c = 40 % for sandstones and ϕ_c = 65 % – for chalks.

Account for critical porosity in the Gassmann's class of the models allows closer approximation of velocity vs. porosity trend over the entire range of porosity, with modified mixture relation, in which the mixed components are the pure solid on one end, and a critical suspension on the other.

Thus, extended low frequency Gassmann's model for velocity vs. elastic rock & fluid properties is not required any more assuming (1) about homogeneity of rock matrix and has the target phenomenon pore pressure included implicitly in the term "P_Δ". Thus, it operates now with the set of new independent rock properties: $K_p(P_\Delta)$, $C_p(P_\Delta)$ and ϕ_c.

2.3. High frequency Biot's model

The requirements for new independent parameters to be included into model attributes for seismic velocities representation increase at higher (ultrasonic) frequencies band.

Assumptions (3) and (4) of F. Gassmann's (1951) theory are violated at higher frequencies. In 1956 M. Biot developed a theory (*Biot*, 1956) relating the elastic properties of liquid-saturated porous rocks to those of dry rocks to account for these high frequencies. In addition to Gassmann's assumptions (1), (2) and (5), Biot assumed that the pore liquid is viscous and relative motion between solid and pore liquid exists and follows to Darcy's law. At low frequencies, Biot's theory reduces to that of Gassmann.

At high frequency, equations (3-3*) for V_p and V_s become frequency depended (*White*, 1983) in agreement with velocity dispersion, which in turn depends on attenuation mechanisms (*King et al*., 2000). In addition Biot's theory predicts the existence of two *P*-waves travelling at different velocities (fast and slow waves) and one *S*-wave. The faster of the two *P*-waves represents the case of the porous matrix and pore liquid being compressed simultaneously, whereas the slower *P*-wave represents the case of one phase being compressed as the second one dilates.

Extending of the frequency band and corresponding generalisation of poro-elasticity theory naturally leads to including into the relevant poro-elastic models new and new parameters to describe fluid relative to solid part motions. The most significant modifications pretend to account for: squirt flow mechanisms (*Dvorkin, Nur*, 1993), phase mixture within the pore space (*Mehta*, 1983), complex pore geometry and composite pore fluid (*Toksoz et al*., 1976; *Berryman, Milton*, 1988), relaxation of viscoelastic memory in coupling modulus (*Carcione*, 1998), high anisotropy of the fractured source rocks (*Vernik, Landis*, 1996) and so on. Some of these models could only reveal themselves within the ultrasonic frequency band. Some of them, like Berryman's and Vernik's models seem to add more model driven non-uniqueness into the velocity value interpretation at seismic work frequency band.

It is important to stress that pore pressure term included in the Biot model to account for relative solid – fluid pore scale motion during propagation of a seismic wavelet belongs to the specifically high frequency phenomena. Certainly this "pore pressure" differs from the target phenomenon included implicitly into the Gassmann's model as in situ sedimentation rock parameters: $K_p(P_\Delta)$, $C_p(P_\Delta)$.

2.4. Discussion

The theoretical models reviewed above include a wide range of porous rock system properties to get the description of elastic modulus suitable for computing of the relevant *theoretical* seismic velocity response. Therefore, over hydrostatic pressure impact on velocity even for rather speculative Earth model is not independent but mixed with other ones. Namely with: rock mineral elastic modulus; integral matrix properties (clay content, anisotropy, grain packing structure, etc.); porosity, pore space geometry (pore spectrum); pore fluid content (saturation, elastic property and viscosity for each phase of pore fluid). The lower is frequency band the bigger is a representative volume of rock to be described and consequently the more effective (volume averaged) supposed to be the relevant model parameter. Thus, the number of Earth model parameters in velocity description cannot be generally predefined exactly. Furthermore, not all of them are independent. It is important to keep this fact in mind while discussing extraction of target over pressure effect from seismically derived velocity parameters.

Theoretical models of the pore pressure controlled acoustic properties for saturated rocks have been described in a number of papers (*Kuster, Toksoz*, 1974; *Toksoz et al*., 1976; *Berryman*, 1980; etc.). These theoretical approaches demonstrate that the appearance – closure of micro-cracks and loose grain contacts in the rock skeleton is the dominant factor in the variation of acoustic properties with pressure for well-grained rock matrix. But the models generally require reliable values of external parameters in order to carry out the forward problem solution. For example, Cheng and Toksoz's theoretical approach (*Cheng, Toksoz*, 1979) requires a pore aspect ratio spectrum to model velocity response. This method can be used in order to establish pore spectra from inversion of measured ultrasonic velocities. G. Tao, M. King and M. Nabi-Bidhendi (1995) showed that, although the resolution of the inversion scheme was generally good, there were departures between the model curve and the experimental results, particularly at lower pressures (< 20 MPa).

Thus, the main source of parametrical information about the links between seismic compressional and shear velocities remains lab experiments on ultrasonic frequencies.

3. Review of empirical models for seismic velocity at different rock lithology

Every theoretical model describing seismic velocity as an inherent rock property includes confining pressure as an important requisition or external condition to determine velocity value numerically. At that, there is some set of additional model properties sensitive to this value, which must be predefined at a certain level, in particular, pore fluid composition, anisotropy, clay content, etc. Often, it is impossible to distinguish each specific contribution on total velocity value based on seismic investigation of in situ rocks. Thus, the lab measurements of seismic velocity vs. confining pressure at other core attribute fixed are the only sources for evaluation of pure "pressure response" on seismic velocity for different kinds of rock lithology. Note, that lab measurements are normally performing on ultrasonic observation systems enabled to simulate dray and partial saturation cases in rock samples at the wide range of confining (dry case) and differential (wet case) pressure: 0-200 Mpa, which corresponds to workable depth interval. Still, the work seismic frequency band is rather shifted to low frequency domain. As a result lab based measurements generally give over-estimations of the relevant parameters. One of the common trick in overcoming this problem consists in using measurements for dry rock samples and then convert the relevant dray moduli (or velocity) into wet ones by using Gassmann's model (*Pennington et al*., 2002).

The importance of pore (P_p) and confining (P_c) pressures on compressional-wave (V_p) and shear-wave (V_s) velocities in various types of sedimentary rocks has been reported by *H. Brandt* (1955), *M. Wyllie et al.*

(1958), *C. McCann, J. Sothcott* (1992), *G. Tao et al.* (1995), *A. Khaksar et al.* (1999) and many other authors. The seismic velocities were found to be sensitive to the differential pressure (P_Δ) or effective stress (P_E). Note that these characteristics are not precisely equal. The first one can be rather easy simulated in lab measurements for dray and partially saturated porous rock (sandy rock), whereas the second one is more like in situ environmental property of the Earth model. In particular, *M. Prasad, M. Manghnani* (1997) suggested that the effects of P_c and P_p are not equal and opposite through the depth. Thus, effective stress (effective pressure – P_E) is used to define conditions when P_p does not exactly cancel P_c:

$$P_E = P_c - \beta P_p, \tag{6}$$

where β is the Biot parameter or *Compression Factor* regulating grain to grain contact changes with the depth (z) and varying from 1.0 at the surface down to 0.7-0.6 at about 5 km (*Christensen, Wang*, 1985; *Prasad, Manghnani*, 1997). According to (*Katsube, Caroll*, 1983) the compression factor can be determined as the following:

$$\beta(z) = 1 - C_s/C_b(z), \tag{7}$$

where C_s and $C_b(z)$ – the skeleton and the bulk rock matrix compressibility, respectively. Thus, the differential pressure P_Δ in contrast to effective pressure P_E can be defined as a special case when $\beta(z)$ is constant and equal to 1.

Unfortunately, most of the empirical works were and are focused on brine and HC saturated or dry sandstones. The carbonates and clay lithology are still remaining in some shade because they are not considering to be exploration targets. So, the pore pressure response for this kind of rocks could indirectly be assessed via empirical velocity – porosity – effective stress relationships (*Hubbert, Rubey*, 1959; *Hattmann, Johnson*, 1965; *Smith*, 1971).

Below we review and analyse published data available about direct empirical links between seismic compressional velocity (V_p) established for sandy rocks in lab experiments and well proven velocity – porosity – effective stress links empirically established for mudrocks in both in situ and lab experiments. This allows us to evaluate rank of pure pore pressure response ideally available in compressional seismic velocity (purified ODVR) against the relevant overpressure anomaly at different lithology and depth.

3.1. Sandy rocks

The empirically available response of seismic velocities to effective stress and partial gas saturation in sandy rocks are well highlighted in the rock physics literature. *M. Wyllie et al*. (1956) showed that, for water-saturated Berea sandstone, *P*-wave velocity increases as effective stress increases. Experimental work by other authors (see, for example, *King*, 1966; *Garanin*, 1970; *Han et al*., 1986; *Yu et al*., 1991; *Freund*, 1992; *Tao et al*., 1995; *Best*, 1997; *Khaksar, Griffiths*, 1999) has shown similar relationships between effective stress and wave velocity for different rocks.

The empirically driven velocity-differential stress relationship ($Vp/s \leftrightarrow P_\Delta$) in consolidated sandstones is non-linear and can be characterised by initial rapid increase in velocity with further reduction in its rate and flattening as it is shown in Fig. 1. Here all samples display quite sharp, exponential increase in the V_p velocities over the range of effective stress from 0 MPa up to 15-30 MPa observed for low and moderate porous sandstones at a seismic frequency band. These results are in good agreement with the ones achieved by *M. Prasad, M. Manghnani* (1997), *S. Domenico* (1976), *C. Yin et al*. (1992), *N. Christensen, H. Wang* (1985), *J. Khazanehdari et al*. (1998) and *M. Zimmer et al.* (2002) for the fine grained dry and brine saturated sandstones with porosity level about 0.40-0.43. The increase in velocity with effective stress is attributed mainly to closure of low aspect ratio pores such as micro-cracks and loose grain contacts in the rock skeleton.

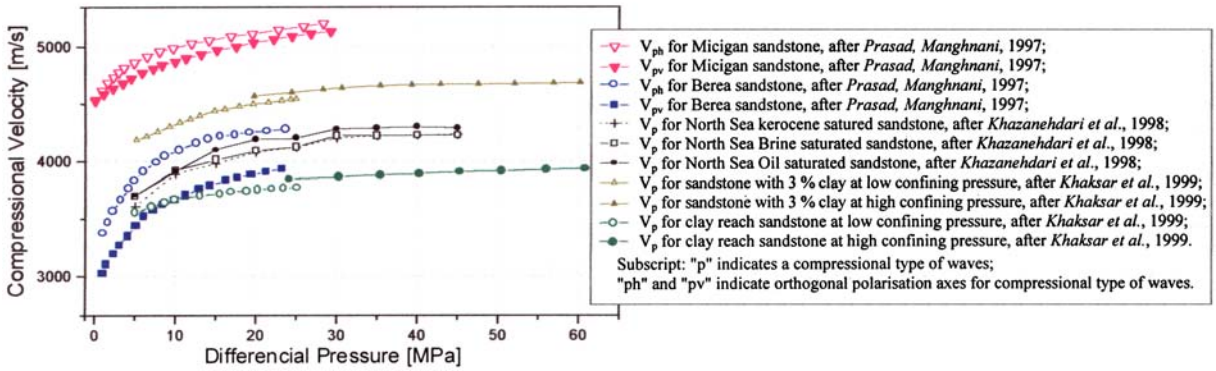

Fig. 1. Empirical relationships between compressional seismic velocity (V_p/*ph*/*pv*) and differential pressure (P) based on published lab measurement results achieved for sandstones

The stress level at which the velocity gradient decreases markedly is known as "microcrack-closure stress", and the corresponding velocity is denoted as "crack-free velocity" (*Eberhart-Phillips et al*., 1989). The magnitude of the microcrack-closure stress is not the same for all rock samples and varies as a function of their porosity and pore space fabric. Above microcrack-closure stress, the velocity varies approximately linearly (close to constant velocity level) with pressure scale, indicating that the micro-cracks were largely closed. At higher confining pressure P_c, the change in slope at the elbow region of the V_p-curves shifts toward higher P_p-values. Furthermore, the change in slope is more gradual at higher P_c. It means that the pure overpressure effect on the V_p parameter expected to be subsiding with the depth at other equal conditions.

A sharp non-linear increase in V_p response at the low effective stress level allows to conclude that the elastic rock properties (in particular, compressional and shear wave velocities) practically become sensitive to the over hydrostatic pore pressure from close to hydraulic fracturing pore pressure level (P_F) (or microcrack-closure stress – P_{mcs}) (*Mathew, Kelly*, 1967). Consequently, the pore geometry and the nature of grain contact should be more important than total porosity in describing V_p versus P_Δ and/or P_E variability with the depth at the given lithology.

Some authors (*Eberhart-Phillips et al*., 1989; *Freund*, 1992) demonstrated that the V_p vs. P_Δ relationship for well grained sandy rocks could be expressed with the following empirical equation consisting linear and exponential parts:

$$Vp/s(P_\Delta) = A - KP_\Delta + B\exp(-DP_\Delta). \quad (8)$$

More recent investigation (*Khaksar et al*., 1999) showed, however, that the term K controlling linear slop in V_p vs. P_Δ relationship is not statistically consistent for well grained sandstones on wide pressure range. In particular, these authors suggested using empirical equation (8) in the simplified form:

$$Vp/s(P_\Delta) = A + B\exp(-DP_\Delta), \quad (8^*)$$

since it gives better fit to the measured velocities with improved prediction of velocities at high confining stresses compared with former (8). Being linear functions of core porosity below the critical porosity level the terms A, B and D in (7) can be empirically derived from the relevant linear regression and/or polynomial fits (see Fig. 2).

Existence of regularity in velocity-differential stress relationships for dray and for partially saturated sandstones allows to substitute the heavy multi-parameter theoretical velocity model by empirically derived approximations.

The remarkable point on the velocity-stress curve, where V_p becomes approximately equal to the crack-free velocity (R), corresponds to the microcrack-closure stress P_{mcc} or the hydraulic fracturing pore pressure limit (P_F). Above this level (pore pressure is ranged between hydrostatic and moderate overpressure) the sandy rock matrix behaves as a monolith skeleton without any noticeable changes in elastic modulus. Below this level, where pore pressure is close to hydraulic fracture limit, the sandy rock matrix looses integrity and its elastic properties are getting remarkably changed.

According to *L. Vernik* (1997) the micro-crack closure stress P_{mcc} is different for different rocks and sediments and is very depended on the porosity level, pore space fabric and clay content. P_{mcc} may increase with decreasing porosity (i.e. for greater depth, consolidation, etc). For example:

P_{mcc} = 100 Mpa for granite (porosity = 0.7),
P_{mcc} = 60 Mpa for tight gas saturated sandstone (porosity = 0.1),
P_{mcc} = 20 Mpa for Ottawa sandstone (porosity = 0.38).

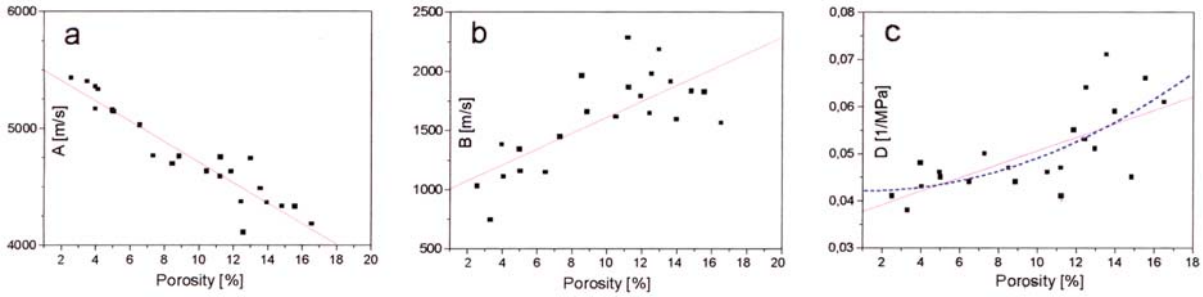

Fig. 2. Polynomial fits established empirically for coefficients in equation (6) and core porosity (based on the data presented by *Khaksar et al*., 1999)

Parameters of linear fit given by (Y = a + b1 X):

(a) a = 5600 ± 70, b1 = - 88 ± 7, R_{square} = 0.890,
(b) a = 940 ± 140, b1 = 67 ± 14, R_{square} = 0.554,
(c) a = 0.036 ± 0.003, b1 = 0.0014 ± $3\cdot10^{-4}$, R_{square} = 0.486.

Parameters of parabolic fit (dashed line on "c") given by (Y = a + b1 X + b2 X^2):

(c) a = 0.042± 0.007, b1 = (-1.918 ± 0.0017) $\cdot10^{-4}$, b2 = (8.8 ± 0.9) $\cdot10^{-5}$; R_{square} = 0.509.

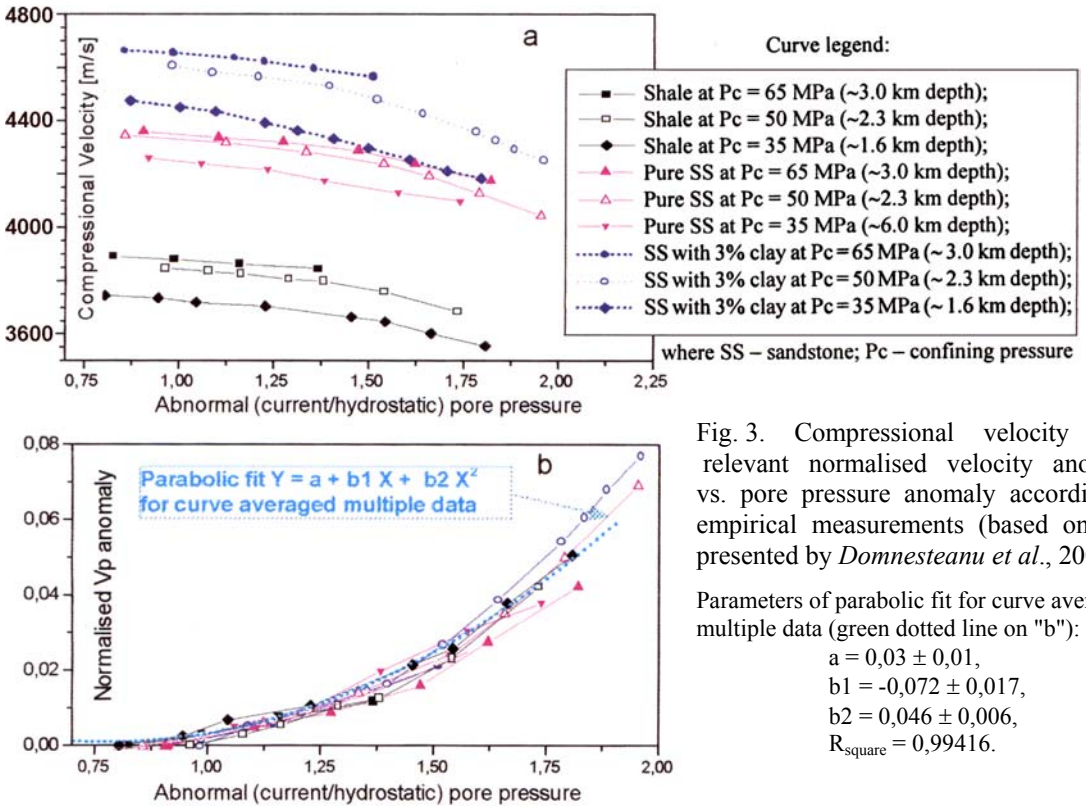

Fig. 3. Compressional velocity (a) and relevant normalised velocity anomaly (b) vs. pore pressure anomaly according to lab empirical measurements (based on the data presented by *Domnesteanu et al*., 2000).

Parameters of parabolic fit for curve averaged multiple data (green dotted line on "b"):
a = 0,03 ± 0,01,
b1 = -0,072 ± 0,017,
b2 = 0,046 ± 0,006,
R_{square} = 0,99416.

In 1999 *A. Khaksar*, *C. Griffiths* and *C. McCann* also showed that at the low confining stress (P_c), high porosity and permeability sandstone samples show greater velocity – effective stress gradient ($\Delta V_p/\Delta P_E$). For example, at 10 MPa confining stress and 15 % porosity velocity gradient is twice higher than at 4 %. Basing on their results we have established linear regression links between best-fit coefficients A, B and D in formula (8*) and porosity within the range 0-20 %, that covers most of questionable from overpressuring point of view in situ reservoir ranges (see Fig. 1-3). It is important to stress that the empirical formula (8*) arranged with appropriate fits formulas for coefficients A, B and D allows evaluation of pure differential stress impact on V_p velocity for sandstone samples at certain range of its porosity.

In agreement with the target overpressure phenomenon it is important to convert commonly used plots from absolute scales V_p versus P_Δ (Fig. 1,3a) to normalised velocity anomaly scales: $\lambda = (V_p - R)/R$ versus normalised overhydrostatic anomaly scales: $\xi = (P_P - H)/H$. Here R is the normal (crack-free) velocity (8*) expectable as a normal case (i.e. as a hydrostatic pressure regime); H is the hydrostatic pore pressure given at any specific depth z by $H = gz\rho_f$, where g – the gravity acceleration; ρ_f – the pore fluid density. It could be done according to (6) by the following substitution of argument: $P_\Delta = P_c - \xi H$.

Let now V_p be equal to the crack-free velocity measured at hydrostatic pressure at shallow depth, where differential pressure approximately coincides with effective stress, i.e. $\beta = 1$ in formula (6). As pore pressure starts exceeding over hydrostatic level, the differential pressure will respectively decrease at any given confining pressure level and compressional velocity will follow one of the empirical curve depending on sandstone type and its current porosity. Thus, pure overpressure effects (ODVR) could be estimated for the given sandstone at any given porosity as it is shown in Fig. 3b.

The achieved multi-curves parabolic fit function coincides with special case of empirical formula suggested by *M. Landro* (2001) to fit normalised velocity response in sandstone ($\Delta V_p/V_p$) to the relevant changes in pore pressure (ΔP) and HC saturation (ΔS):

$$\Delta V_p/V_p = m_1\Delta S + n_1\Delta P_p + n_2(\Delta P_p)^2. \qquad (9)$$

Evidently in our particular case $\Delta S = 0$. This allows estimation of pure ODVR for sandstone as averaged over available sandy rock samples function of porosity and depth (see Fig. 3b and Fig. 8c).

In practice however such purified effect can never be achieved. As it is reported by many authors (*Gardner et al*., 1974; *Domenico*, 1976; *Brown, Korringa*, 1975; *Yin et al*., 1992) the measurable effect of partial HC (especially gas) saturation of composite pore fluid on V_p and V_s velocities in well-grained reservoirs can be comparable and even can exceed the effective pressure impact from rather low saturation range (2-5 %). In particular, for gas saturated sandstones on moderate depth about 1500-2500 m the value of V_p can be reduced on

20 % against its normal range (*Gregory*, 1976). The average range of magnitude of the gas saturation effect on compressional waves' velocity is illustrated on composite plot shown in Fig. 4, which summarises lab studies for high porous (20-28 %) sandstones with low clay content (10 %) reported by (*King et al.*, 2000).

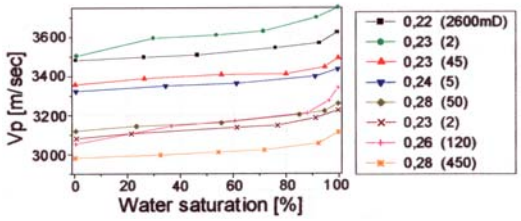

Fig. 4. Empirically derived curves approximating link between compressional seismic velocity (V_p) and water saturation for sandstones (*King et al*., 2000).
Curve code: $N(M)$, where N – porosity value [%], M – permeability value [mD]

3.2. Mudrocks (clays and shale)

Despite of the fact that mudrocks comprise more then 70 % of the geological space within the sedimentary basins their elastic properties are significantly less investigated mainly because they are not represented principal oil and gas reservoirs. It is generally agreed (*Tosaya*, 1982; *Dewhurst et al*., 2000; *Lahann et al*., 2001) that the seismic velocity response on effective stress decreasing follows the same feature like for sandstone (see also Fig. 1-3). At the same time, clay bearing rocks reveal much higher level of plasticity and anisotropy during burial and diagenesis history (*Vernik*, 1994; *Vernik, Landis*, 1996; *Sejourne et al*., 2000). On the one hand, these factors mask the pure overpressuring effect on seismic velocity for in situ measurements in mudrocks and increase uncertainty of the relevant velocity anomaly. On the other hand, the natural porosity reduction with depth according to normal compaction trend (*Reike, Chilingarian*, 1974) is much more evident and predictable than the relevant phenomenon for sandstone. It allows to utilise a triple link "effective stress – porosity – compressional velocity" to establish the relevant empirical relationships ($Vp/s \leftrightarrow P_E$) for mudrock (*Hubbert, Rubey*, 1959; *Smith*, 1971; *Dutta*, 1983).

Note, that this commonly approved porosity based approach ("Porosity Tool") for clay-shale-silt (mudrock) lithology implicitly implies combining of two independent petrophysical relationships: first – between seismic velocity and porosity ($Vp/s \leftrightarrow \phi$); second – between porosity and effective stress ($\phi \leftrightarrow P_E$). Both approaches are well addressed in literature (see, for example, reviews by *K. Magara* (1978), *J. Mouchet and A. Mitchell* (1989), *N. Dutta* (2002a,b)). Below we briefly compile the main ideas and formulas needed for further estimation of empirically based OVDR and simulations some typical case scenarios.

3.2.1. Compaction vs. effective stress models

The mechanical compaction of mudrock during burial is normally associated with micro-scale matrix repacking and releasing of pore water in response on increase of total sediment load (*Magara*, 1978). In tectonically relaxed sedimentation environment this process can be well approximated within the range of Terzaghi's one-axial effective stress model (*Terzaghi, Peck*, 1948), which is represented by (6) in the form corrected for secondary porosity reduction mechanisms. The relevant porosity reduction as a measure of compaction can be represented via exponential function of current depth (Athy-like trend) – $\phi(z)$ (*Athy*, 1930) or current effective stress – $\phi(P_E)$ (*Hubbert, Rubey*, 1959; *Palciauskas, Domenico*, 1989):

$$\begin{cases} \phi(z) = \phi_0 \exp(-Hz); \\ \phi(P_E) = \phi_0 \exp(-KP_E), \end{cases} \tag{10}$$

where z and P_E are the independent arguments – depth and effective stress, respectively; $\phi(z)$ /$\phi(P_E)$ and ϕ_0 are the current and initial porosity, respectively; the compaction coefficient H and K are linked via bulk density of the sediments and the density of pore water (*Luo, Vasseur*, 1992) (see also Appendix).

Regardless of modification (*Smith*, 1971; *Dutta*, 1983; 1987; *Bowers*, 1995), equation (10) defines some bijective operator for conversion of equivalent depth (*Magara*, 1978) or effective stress (*Eaton*, 1972) anomaly to porosity anomaly and back on the condition that the one-axial stress model (6) is valid.

In practice the validity of effective 1-D models (6) and (10) for both effective stress and the relevant porosity response is seriously restricted within intervals of young continuously subsiding part of sedimentary sections represented by homogeneous mudrock lithology with predominantly one-axial (along depth axis) load during sedimentation history. Indeed, 1-D mechanical compaction equilibrium models (10) based on one-axial Terzaghi's stress model (6) ignores non-vertical components of the effective stress (lateral stressing) or/and also non-vertical components of releasing fluid flow (centroid effect (*Traugott*, 1996)). It also does not account for any secondary porosity reduction or/and secondary fluid generation phenomena like clay mineral conversion or/and Kerogen degradation phenomena (*Meissner*, 1981; *Swabrick, Osborne*, 1996). Thus, oversimplified compaction model (10) is potentially highly non-unique when it is used for data fitting and then for recovering of effective stress anomaly from porosity anomaly.

For example, consequent repeated cycles of effective stress increasing-decreasing in lab measurements or during subsidence-erosion (loading-unloading) cycles at natural sedimentation reveal visible hysteresis in ϕ vs. P_E and consequently V_p vs. P_E curves (*Karig, Hou*, 1992). The nature of these phenomena consists in the way of stress releasing. Indeed, there are two possibilities for reducing of difference between confining pressure and pore pressure: first – by increasing of pore pressure, second – by decreasing of confining pressure. The first scenario corresponds to loading limb while sedimentation in nature, when some excess hydrostatic pressure can develop due to combining of fast sedimentation rate and rapid decreasing of pore fluid conductivity through the mudrocks. At this, overpressuring is accompanied with departure of porosity vs. effective stress trend from mudrock normal compaction curve (*Magara*, 1978). Abnormally high porosity correlates with abnormally low V_p velocity. The second scenario corresponds to the unloading limb associated with erosion episode in sedimentation history. At this, mudrock reveals irreversible behaviour of the plastic deformation during rock matrix compaction. Thus, V_p value at the same level of effective stress can be much higher then V_p value for the same rock following to loading limb (*Tosaya*, 1982). In order to get unique conversion for V_p based on link (10) it is necessary to recognise to which limb the relevant part of the section belongs.

Clearly, that this problem is redoubled in times with the age of exploration target.

In addition to non-unique reversing of formula (10), this operation is also non-stable as it is shown in Fig. 5.

Indeed inversion of (10) gives the following formula for recovering of current effective stress:

$$P_E = [\ln(\phi_0) - \ln(\phi)]/K. \qquad (11)$$

Then sensitivity of effective stress to changes in porosity is getting as

$$\partial P_E/\partial\phi = -1/\phi K. \qquad (11^*)$$

Clearly, that a small perturbation in porosity corresponding, for example, to aimed departure from normal compaction trend will result in infinite changes in recovering effective stress when porosity value is approaching to zero. Thus, instability in using any of Eaton-like method for overpressure prediction (trend based Porosity Tool) will hyperbolically rise with the depth.

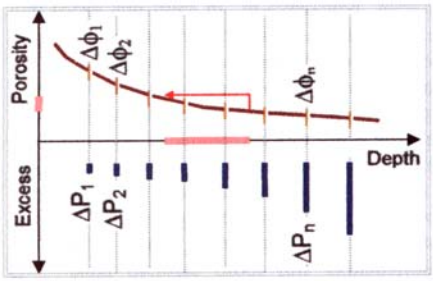

Fig. 5. A speculative example of non-stability of Porosity Tools for overpressure estimation which occurs at great depth. The equal porosity perturbations (transparent strips on "Porosity vs. Depth" plot) are converted against exponential compaction trend into the "overpressure responses" increasing with depth (bold strips on "Excess pressure vs. Depth" plot).

There is range of corrections in both one-axial stress model (6) and porosity reduction formula (10) aiming for reducing of mentioned non-uniqueness.

G. Bowers in his approach suggests extension of Eaton's method on cases, where overpressure could be caused not only by compaction disequilibrium (*Bowers*, 1995). Still, this method implies alternative "unloading normal trend" line besides "loading normal trend" to be examined and fitted against offset well.

Thus, it remains to be pure empirical one (i.e. it is part of Porosity Tools) and it does not take the non-uniqueness problem away since the answer on question "which trend from available should be used for conversion?" at any particular case depends on the user intuition and common sense.

The correction for non-scalar origin of the effective stress field implies substitution of effective (vertical) stress value in (10) on the mean stress value approximated as the following (*Alberty, McLean*, 2003):

$$P_{\text{mean}} = (P_E + P_{H\min} + P_{H\max})/3, \qquad (12)$$

where P_{mean} is the mean stress; P_E – the vertical component of total stress; $P_{H\min}$, $P_{H\max}$ are the estimations of minimal and maximal components of horizontal stress. The vertical stress is normally easy determining from integration of density or pseudo-density logs. The minimum horizontal stress could be estimated from leak-off tests in a few in situ measurements. The maximum horizontal stress cannot be measured directly, but could be only approximately inferred from structure geology and well bore response. Using mean stress instead of vertical one in Eaton-like data driven models appears to be obligatory within the tectonically active sub-surface environments (*Yassir, Bell*, 1994).

The correction for secondary porosity reducing mechanisms normally extends mechanical compaction model (10) by introducing temperature argument in addition to stress into exponential function (*Dutta*, 1983) or power law function (*Baldwin, Butler*, 1985).

There is one important feature in common for all of these extensions: the attempt to use the bijective trend operator (Porosity Tool) for approximation rather complex and multi-mechanisms process, which is the mudrock compaction process in nature. Thus, validity of any Porosity Tool remains ultimately limited by 1-D static assumptions.

3.2.2. Compressional velocity vs. porosity models

The gradual increase of seismic velocity is well correlated with the relevant increase in mudrock solidity defined as $(1 - \phi)$. It allows to use Voigt – Reuss type of averaging formula (5) for establishing the relevant fit function. The simplest of them is classical time-average Wyllie's equation (*Wyllie*, 1957) relating porosity to seismic slowness (or transit time – $\Delta\tau$), namely:

$$\Delta\tau = (1 - \phi)\Delta\tau_s + \phi\Delta\tau_f, \tag{13}$$

where $\Delta\tau_s$, $\Delta\tau_f$ are the slowness of seismic waves propagating through the solid and fluid part of a mudrock, respectively. Similar time averaging formulas (*Pickett*, 1963; *Issler*, 1992) imply linear approximations of transit time data. This approach with some correction for lithology variations is commonly used for converting sonic data into porosity scale.

There is range of non-linear empirical functions specifically oriented on fitting of compressional velocity trend with normal compacted porosity trend in mudrocks.

Geertsma's equation is valid for consolidated mudrocks at the porosity range below Critical Porosity (*Geertsma*, 1961):

$$V = [(u_f + u_s)/\rho_b]^{1/2}, \tag{14}$$

where

$$u_f = (1 - C_b/C_s)^2/[C_b(1 - C_b/C_s - \phi) + \phi C];\ u_s = 1/C_s + 3Y_s^S/4;\ \rho_b = \rho_s(1 - \phi) + \rho_f\phi;$$

V – the compressional seismic velocity [km/s]; C – the compressibility [Mpa^{-1}]; Y^S – the young shear module given by $Y^S = \rho\,(V^S)^2$; V^S – the shear seismic wave velocity module, ρ – the density [g/cm^3]; ϕ – the porosity [fraction]. Subscripts s,f denote the solid and fluid part of sample rock volume, respectively.

Still the more common for mudrock lithology is simpler Raiga-Clemenceau's equation relating velocity and porosity at wider porosity range (*Raiga-Clemenceau et al*., 1988).

$$\phi = 1 - (V/V_m)^{1/X}, \tag{15}$$

where V_m – the matrix velocity ($V_m \sim 4.5$ m/sec works for US Gulf of Mexico shale); X – the lithology dependent exponent ($X \sim 1.19$ for the Gulf of Mexico shale).

The porosity derived depth trends for compressional velocity were computed based on Wyllie's model (13), Geertsma's (14) and Raiga-Clemenceau's (15) equations tuned to Tertiary mudrock conditions of Western Siberia (see s/section 5.2.3). They are plotted in common in Fig. 6.

Another well-proven relationship is Gardner's equation (*Gardner et al*., 1974) which is also often used to obtain density from velocity.

$$\rho_b = AV^B, \tag{16}$$

where V and ρ_b are the compressional seismic velocity and bulk density defined above for formula (14); A and B – the lithology dependent coefficient and exponent ($A \sim 0.235$ and $B \sim 0.25$ for the Gulf of Mexico shale).

The bulk density values obtained from velocity by using (16) can then be integrated with the water column to provide overburden stress (confining pressure – in lab measurements or geopressure – in situ assessments) at any given depth level by the following integration:

$$P_C(Z) = g\int_0^z \{\rho_s(1 - \phi(z)) - \rho_f\phi(z)\}dz, \tag{17}$$

where g – the gravity constant and Z – the current depth.

Finally, the velocity derived overburden pressure (17) could then be used in one-axial Terzaghi's stress model (6) for conversion of velocity anomaly into overpressure response.

The normalised velocity response in mudrock ($\Delta V_p/V_p$) on the relevant changes in pore pressure (ΔP) will be considered as a function of depth together with the relevant sandstone signature in the next subsection.

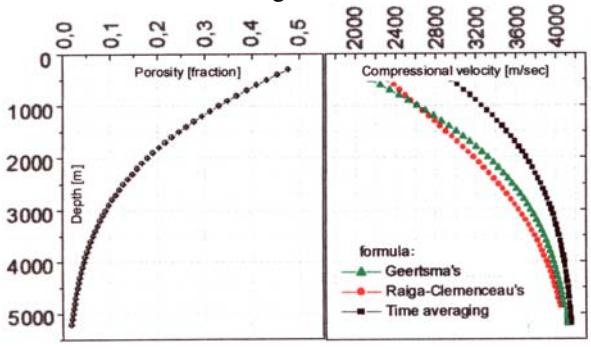

Fig. 6. Velocity vs. depth trends (right) computed for single normal compaction porosity depth trend (left) in agreement with conventional empirical relationships indicated on velocity curve legend (formulas: 13-15).

As to the inherent mudrock factors, which could disguise the target velocity anomaly – they are different from ones in sandy rocks. The most important perhaps is an impact of shale anisotropy. The shale anisotropy is especially strong for source rocks, where it is commonly recognised to be originated from strict laminating and fracture orientation while burying, diagenesis and primary HC generation (if they are matured enough) (*Vernik*, 1994; *Vernik, Landis*, 1996). This effect on seismic velocity value in shale may reach up to 10-15 % (*Sejourne et al*., 2000) without significant changes with the depth due to increasing anisotropy with decreasing porosity.

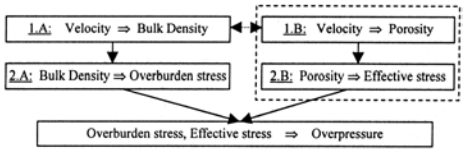

Fig. 7. The generic work flow scheme for velocity-overpressure conversion process. The dashed rectangular frames two blocks combined into one for sand lithology

3.3. Discussion

Considered empirical relationships established for sand and clay-shale lithology are well proven and form solid empirical basis for seismically driven overpressure prediction all over the world (*Dobrynin, Serebryakov*, 1978; *Mouchet, Mitchell*, 1989; *Huffman*, 2002).

As it follows from the background speculative (6-7,9) and empirical models (8,10-17) the extraction of target anomaly (ODVR) remains to be uncertain and non-stable even for quite ideal conditions.

Let us now summarise the empirical relationships reviewed for sandy rock and mudrock lithology into generalised work flow diagram showing some typical routine required for converting available velocity anomaly into target overpressure anomaly.

Note that the sand lithology implies two steps' algorithm: 1 – "velocity-effective stress", 2 – "effective stress – overpressure", whereas the mudrock lithology demands intermediate step to provide a triple link: "velocity-porosity-effective stress" and then use common for both lithologies "effective stress – overpressure" relationship (6).

Thus, the velocity to overpressure conversion scheme for sandy-rock looks simpler and more certain. Indeed, processes 1.B and 2.B are incorporated for sandstone in bijective links (8-8*). However, the range of sensitivity to overpressure changes and magnitude of maximal anomaly for sand lithology are worse than they are for clay-shale lithology because they are closely related to integrity of sand rock matrix and are very different above and below the "crack-free velocity" (see s/section 3.1).

The situation with sensitivity and magnitude of velocity anomaly for clay-shale lithology is softer. The first stage link "Velocity-Porosity" is represented by processes 1(A,B), where process 1.A can be based on Gardner's equation (16); process 1.B implies one of the empirical models described in formulas (13-15). Evidently, the relations established for porosity and bulk density are mutually related.

The second stage link "Porosity – Effective/Confining Pressure" is represented by two parallel processes 2A and 2B. In particular, process 2A includes algorithms (16-17), process 2B implies application of any Eaton-type method grounded on empirical compaction law (10).

The final stage – conversion to the target overpressure anomaly – is common with the sandy rock lithology case. It is based on one-axial Terzaghi's stress model for clay-shale lithology, which coincides with differential pressure model for sand lithology at Compression Factor $\beta(z) = 1.0$ in formula (6).

4. Modelling of ODVR variation with depth in ideal and real clastic rock sections

As the depth level of sedimentary rock increases the contrast and magnitude of the relevant seismic response (ODVR) subside for both compressional and shear wave velocity. The common reason of these phenomena for both sand and clay-shale lithology is shift in compaction process from mechanical mechanisms toward secondary (diagenetical) porosity losses, which become primary important from 2.0-2.5 km in sandstones and 2.5-3.0 km in clay depending mainly on local subsurface temperature gradient (*Luo et al*., 1993; *Kool*, 1997). The stress controlled re-packing process within the pore space below this level is gradually (clay) or sharply (sand) getting replaced with temperature controlled clay mineral diagenesis or crushing-cementation processes, respectively (*Allen, Allen*, 1990). Note that there are at least seven parallel micro-scale processes commonly recognised to be responsible for evolution of pore space fabric during burial history (*Waples, Kamata*, 1993), whereas empirical stress compaction equation (10) has just two adjustable model parameters to fit to the data. Very roughly these processes are accounted for by introducing depth depending Compression Factor $\beta(z)$ into Terzaghi's one-axial effective stress model (6-7), which subsides the sensitivity of ODVR to stress changes due to overpressure variations.

Thus, the empirically driven trends of velocity vs. effective stress provide very gross and smoothed estimation of target velocity response variations with the depth. Still, this is what investigators have as a tool for estimation and prediction of overpressure.

In context of this paper it is important to recognise how sensitive the velocity anomaly (λ) will be to the given in advance target (overpressure) anomaly level – ξ at different depth and lithology based on introduced

above empirical links. To check this we will introduce a target sensitivity measure and we will estimate it as a function of depth based on background relationships (6, 8, 10-17).

Let (by analogy with formalism introduced in s/section 3.1) the normalised V_p velocity anomaly be defined as a function of normalised excess hydrostatic pore pressure anomaly ξ in agreement with the scale in Fig. 3b. $\lambda(\xi) = (V_\xi - V_1)/V_1$, where $\xi = (P_P - H)/H$; H and P_P are the hydrostatic and above hydrostatic pore pressures; V_ξ and V_1 – the normal ($\xi = 1.0$) and abnormal ($\xi > 1.0$) V_p velocities. Let us now fix certain k-th levels of overpressuring between hydrostatic and close to fracture limit as the following: $\xi_k = 1.0, 1.1, 1.2,\ldots 2.0$. Clearly that the relevant levels of effective stress can be recovered from (6) given in the form:

$$P_E(\xi_k, z) = P_c(z) - \beta(z)[\xi_k H(z)], \tag{6*}$$

where function $\beta(z)$ is based on empirical links for Compression Factor (*Katsube, Caroll*, 1983); $P_c(z)$ is getting from weight averaged formula (17) and normal compaction law (10-11) and as soon as fluid & matrix density and compaction constants (for clay only) are assigned.

The aimed relationship for sandstone lithology can uniquely be achieved based on the following consequent scale transformations:

$$\lambda(\xi_k, z) \Leftarrow V\{\xi_k; P_C[\phi(z)]\} \Leftarrow P_E[\phi(z)] \Leftarrow \phi(z) \Leftarrow z, \tag{18}$$

where $\phi(z)$ is defined based on Athy-like porosity-depth trend and sandstone compaction constants calibrated for every particular region (*Madatov, Sereda*, 2000b); $P_E[\phi(z)]$ is given by (8*) with porosity depended coefficients (see Fig. 2); $V\{\xi_i;P_C[\phi(z)]\}$ is given by formulas (6, 17).

The similar relationship for mudrock lithology can uniquely be achieved based on the following consequent scale transformations:

$$\lambda(\xi_i; z) \Leftarrow P_E\{V[\phi(\xi_i; z)]\} \Leftarrow V[\phi(\xi_i; z)] \Leftarrow \phi(\xi_i; z) \Leftarrow z, \tag{18*}$$

where $\phi(\xi_i; z)$ is defined based on Athy-like porosity-depth trend with clay compaction constants calibrated for every particular region (*Madatov and Sereda*, 2000b) and then can be corrected for given excess hydrostatic pressure ξ_i by using the equivalent depth method (*Magara*, 1978); $V[\phi(\xi_i; z)]$ can be given by one of empirical relationships (13-15)[2] (see also Fig. 6); $P_E\{V[\phi(\xi_i; z)]\}$ can be provided by any of available *Porosity Tool* grounded on extended Terzaghi's one-axial effective stress model (6*). The constants necessary for conversion are listed in Table 1. Note that the compaction constants for sand and clay lithology are area depended. Corresponding values are resulted from calibration experience in different sedimentary basins (*Madatov, Sereda*, 2000b).

4.1. Abnormal depth trends for speculative models

The first group of simulations was aimed to reproduce some ideal homogeneous sections represented by pure sandstone or pure mudrock lithology with the model parameters given according to Table 1[3]. The results are represented in Fig. 8. Here the level of the relative velocity response $\lambda(\xi_i; z) = 0.05$ is marked as a typical accuracy threshold (5 %).

There is a maximum in $\lambda(\xi_i; z)$ curves on the depth level about 750-1000 m and 1000-1500 m for sandstones and mudrock, respectively, visible at any value of predefined overpressure anomaly – ξ_i. This apparent maximum of ODVR sensitivity is due to different rate in rising of velocity departure from normal compaction velocity trend (velocity anomaly) and rate in rising of absolute seismic velocity values (trend values) versus depth. This effect is more contrast for sandstones, since their matrix velocity is bigger then ones in clay lithology. The non-linear slope of $\lambda(\xi_i; z)$ curves below apparent maximum is controlled by Compression Factor $\beta(z)$ behaviour and compaction constants for the relevant rock.

The 5 % threshold in the relative compressional velocity for the mudrock section occurs at shallow depth levels up to 2.5 km for overpressure anomaly $\xi \sim 1.35$ g/cm^3 (see Fig. 8b), whereas the same threshold in $\lambda(\xi_i; z)$ for sandstone section starts at much higher overpressure anomaly $\xi \sim 1.5$ g/cm^3 at about 500 m depth with the sharp non-linear increase up to 1.9 g/cm^3 at 2.5 km (see Fig. 8c). The reason for this is quite different mechanisms of sensitivity of compressional velocity to the effective stress reduction in clays (where velocity correlates with porosity losses) and in sandstones (where velocity is getting really sensitive to the effective stress variation only below micro-crack closure level).

According to these simulations the compressional velocity anomaly above 5 % could not be expected below 2.5 km if overpressure anomaly exceeds 1.4 and 1.9 g/cm^3 for mudrock and sandstone sections, respectively. This depth level in average corresponds to one where secondary porosity losses' processes start domination over the primary ones (*Waples, Kamata*, 1993; *Luo, Vasseur*, 1996; *Kool*, 1997).

[2] We have used in our simulations for clay-shale lithology Raiga-Clemenceau's equation (15).
[3] The North Sea case was used for non-global constants.

Table 1. Constants' specification used for simulation of ODVR vs. depth

Parameter - Definition	Value	Unit	Comments	Reference[4]
ρ_f – water density	1020	kg/m^3	Universal constant	(1)
ρ_s – sandstone matrix density	2550	kg/m^3	Global constant	(1)
ρ_s – mudrock matrix density	2650	kg/m^3	Global constant	(1)
ρ_s – evaporite matrix density	2170	kg/m^3	Global constant	(1)
V_M – compressional velocity in water	1480	m/s	Universal constant	(1)
V_M – compressional velocity in evaporite	4900	m/s	Global constant	(1,2)
V_M – compressional velocity for sandstone matrix	5400	m/s	Tertiary section, North Sea	(1,2)
	5600	1/m	Tertiary section, Gulf of Mexico	(3,5)
V_M – compressional velocity for mudrock matrix	4390	1/m	Tertiary section, North Sea	(1,2)
	4540	1/m	Tertiary section, Gulf of Mexico	(3,5)
H – Athy compaction constant for sandstone	0.00025	1/m	Tertiary section, North Sea	(4,6)
	0.00019	1/m	Tertiary section, Gulf of Mexico	(4,6)
H – Athy compaction constant for mudrock	0.00033	1/m	Tertiary section, North Sea	(4,6)
	0.00029	1/m	Tertiary section, Gulf of Mexico	(4,6)
ϕ_0 – surface porosity constant for sandstone	0.55		Tertiary section, North Sea	(4,6)
	0.48		Tertiary section, Gulf of Mexico	(4,6)
ϕ_0 – surface porosity constant for mudrock	0.65		Tertiary section, North Sea	(4,6)
	0.60		Tertiary section, Gulf of Mexico	(4,6)

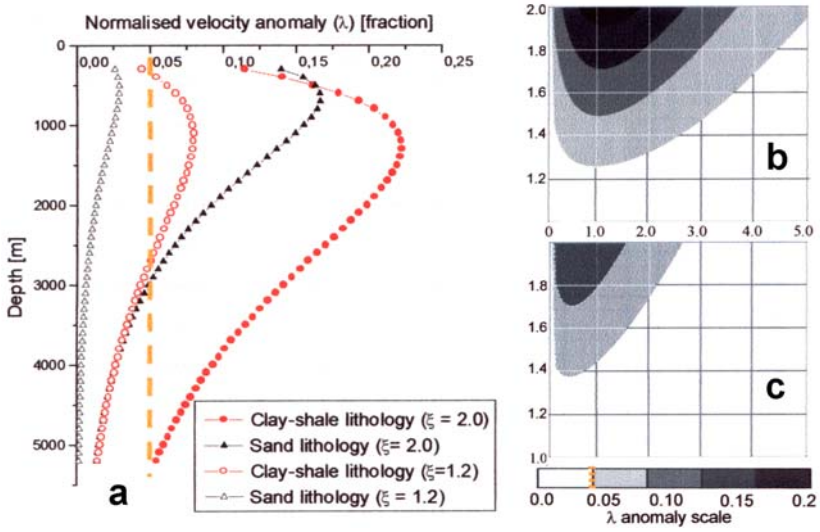

Fig. 8. Depth trend of normalised velocity anomaly (λ) for different excess hydrostatic anomaly level (ξ).
a – combine clay & sand lithology plot λ vs. depth;
b, c – contour plots for clay (b) and sand (c) lithology, respectively.
Horizontal axis – depth [km].
Vertical axis – overpressure anomaly level (ξ).

4.2. Simulations based on real cases

Evidently, the speculative trend based estimations represented in Fig. 8 can only be suitable for very draft analysis. More representative and practically important estimations of the direct velocity response on overpressure anomaly (ODVR) requires more realistic geology setting and more sophisticated models at least for simulation of present day porosity and effective stress profiles. We have used a basin modelling approach and the relevant program package for this purpose.

The extended reviews of the background theory and applications of basin modelling approach are available in many published issues (see, for example, *Allan, Allan*, 1990; *Lerch*, 1990). In connection with the simulation of target phenomena (overpressure, effective stress and porosity) we are referring here on Effective Basin Model approach (see *Madatov, Sereda* in this issue) and overpressure modelling-calibration-prediction PANDA package (*Madatov et al*., 1996b; *Madatov et al*., 1997; *Madatov et al*., 1998; *Madatov, Sereda*, 2000b).

The Effective Basin Model approach aims for generation of invertable basin model from normally available geology settings and well data sets, its calibration and further uses it at real time overpressure prediction. The very general scheme of the relevant program package is shown in Fig. 9.

Here the upper level data sets (1A-C) represent input information required for setting, upscaling and calibration of geo-fluid system models (2A-C) describing at final stage (3) porosity – effective stress and pore

[4] The reference number is given according to the following list: (1) – *Avtchan et al.*, 1979; (2) – *Averbukh*, 1982; (3) – *Gardner et al.*, 1974; (4) – *Luo et al.*, 1993; (5) – *Mello, Karner*, 1996; (6) – *Madatov, Sereda*, 2000a.

pressure evolution during basin time scale. The key computer routine, which provides generation of effective basin model fitted to the available data, indicators and settings is multi-source data inversion (*Madatov et al*., 1997; *Madatov et al*., 1998; *Madatov, Sereda*, 2000a). The basin modelling engine ensures computing of the synthetic data prototype fitted to real data at all calibration well locations and presumably ensures rather accurate for "the first guess" porosity, effective stress and pore pressure curves for the planed well.

This output ideally suits for the purposes of real case simulation of ODVR.

Note, that the type and specification of empirical relationships for converting the basin model output (porosity and effective stress) to the theoretical velocity response depends on region and lithology.

In particular, two geology-empirical settings were used for simulation of target anomaly $\lambda(\xi; z)$: the North Sea and Gulf of Mexico sedimentary basins. The relevant stratigraphy – lithology settings are represented in Fig. 10.

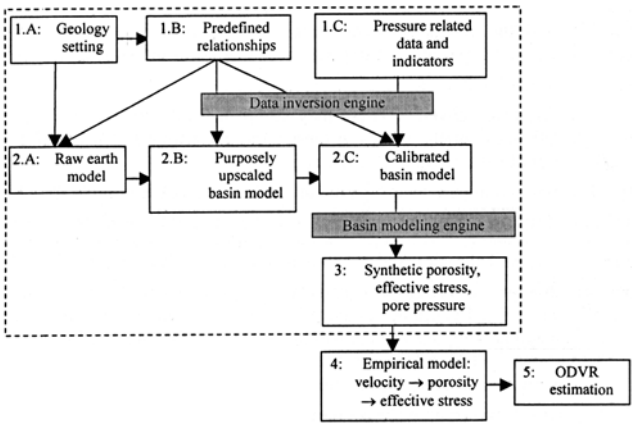

Fig. 9. The generic work flow scheme of basin model derived simulation of seismic velocity response (ODVR). Dashed rectangular frames the blocks attached to PANDA© package

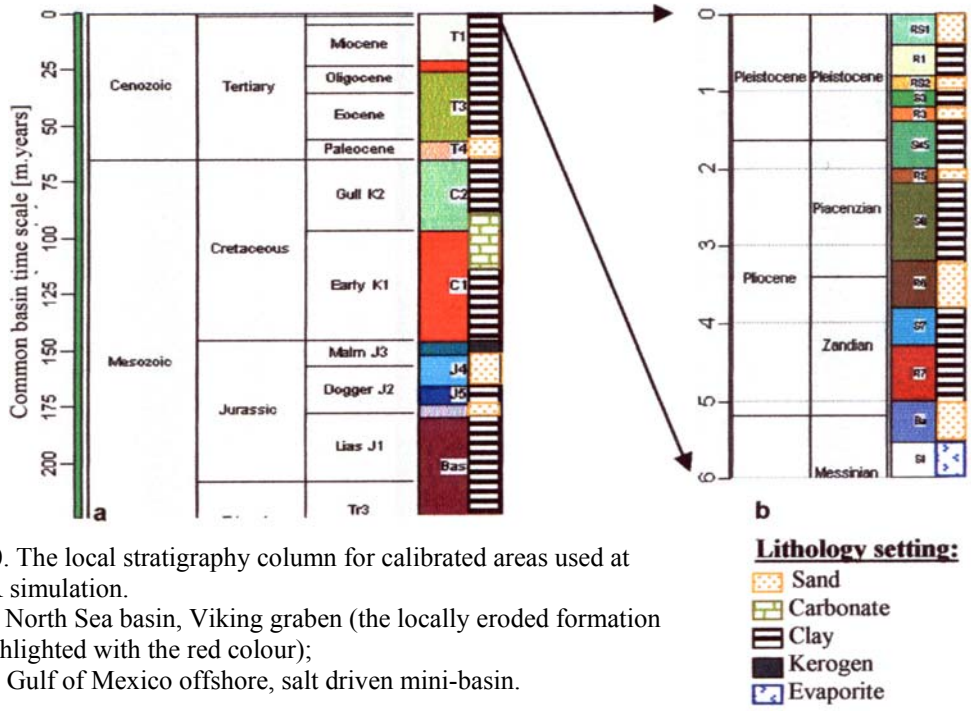

Fig. 10. The local stratigraphy column for calibrated areas used at ODVR simulation.
a – the North Sea basin, Viking graben (the locally eroded formation highlighted with the red colour);
b – the Gulf of Mexico offshore, salt driven mini-basin.

4.2.1. The North Sea example

The column in Fig. 10a represents general for the region sequence of formations which includes: monotonous mudrock Tertiary part; shale-carbonate Cretaceous part with eroded bottom portion regionally recognised as Base Cretaceous unconformity; Jurassic argillaceouse mixture part containing main exploration targets (see (*Introduction to the petroleum geology of the North Sea*, 1984) for more details).

The typical present day overpressure picture in the area contains two abnormal zones: smoothed, moderate by amplitude and poorly recognised from well drilling data "nose" at the bottom part of Tertiary megasequence and high amplitude anomaly below Base Cretaceous unconformity with sharp transition zone (see Fig. 11b). The intermediate Cretaceous part tends to be at hydrostatic regime in North direction from centre of Viking graben (*Chiarelli, Duffaud*, 1980). The upper anomaly could be associated with the single key

mechanism: rapid sedimentation rate during late Tertiary in combination with poor permeable bottom part perhaps affected also with smectite to illite clay mineral transformation (*Lahann et al*., 2001). Whereas there is a bunch of possible overpressure mechanisms combining at developing of the lower abnormal zone. They are: secondary porosity losses in sandstones; gas generation and oil cracking in source rock; pressure communication through deepening aquifer formations and fault compartmentalisation. As a result, the lower abnormal zone is commonly hard for prediction target with mosaic and sharp lateral changes (more detailed review of the overpressuring mechanisms acting in the region is available in the published literature (*Chiarelli, Duffaud*, 1980; *Buhrig*, 1989; *Helth et al*., 1994; *Kool*, 1997)).

There is rather different experience in overpressure prediction within this area by using standard seismic velocity based tools: from very positive (*Carcione, Helle*, 2002) to rather negative (*Campbell et al*., 2000). It is clear that the background one-axial Terzhagi's model is not capable to describe and to explain all observable diversity of target phenomena. Thus, the success of such kind of predictions is always a matter of good luck.

Simulation of compressional velocity response for one of calibration wells in this area is illustrated in Fig. 11. The routine includes full-scale calibration and pressure modelling stages in agreement with the scheme represented in Fig. 9. The burial history and compaction history plots represented in common time scale (Fig. 11a-c) illustrate the final phase in modelling of synthetic porosity and effective stress & overpressure curves. The empirical links (8*) and tuned for the area Raiga-Clemenceau's equation (15) were used for conversion of effective stress and porosity to velocity scale for sandstone and mudrock, respectively.

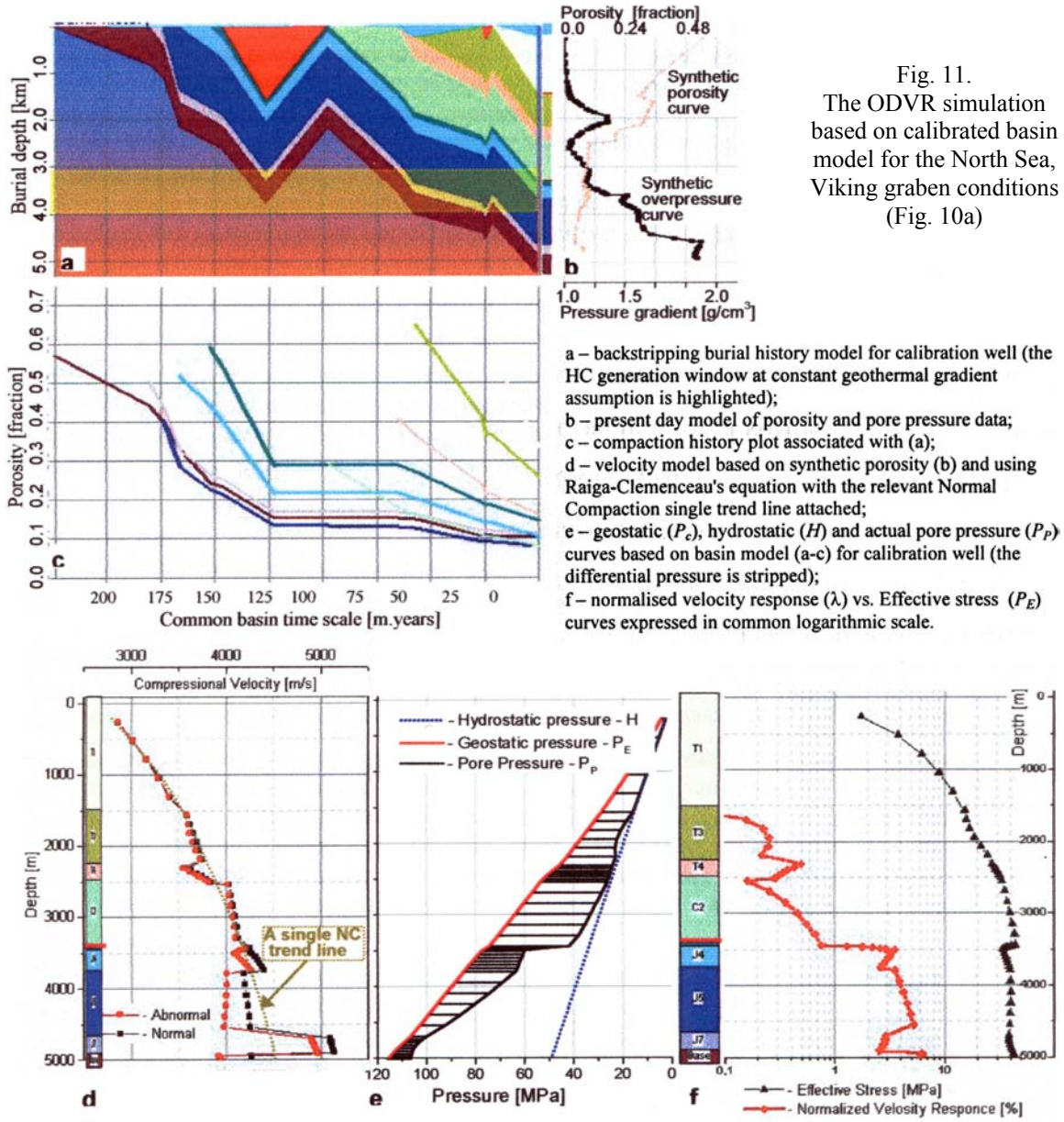

Fig. 11.
The ODVR simulation based on calibrated basin model for the North Sea, Viking graben conditions (Fig. 10a)

a – backstripping burial history model for calibration well (the HC generation window at constant geothermal gradient assumption is highlighted);
b – present day model of porosity and pore pressure data;
c – compaction history plot associated with (a);
d – velocity model based on synthetic porosity (b) and using Raiga-Clemenceau's equation with the relevant Normal Compaction single trend line attached;
e – geostatic (P_c), hydrostatic (H) and actual pore pressure (P_P) curves based on basin model (a-c) for calibration well (the differential pressure is stripped);
f – normalised velocity response (λ) vs. Effective stress (P_E) curves expressed in common logarithmic scale.

As it follows from results displayed in Fig. 11d-f the magnitude of relative velocity anomaly should not exceed 1 % level above 3 km depth. Thus, the undercompaction effect presumably related to upper overpressure anomaly on Tertiary level is not significant enough to evoke noticeable ODVR. In other words, this depth interval entirely belongs to a shadow sensitivity of the target zone. The 5-6 % magnitudes' level of $\lambda(\xi_i; z)$ curve is reached within the Jurassic sandstone – mudrock interval at depth level 3.5-4.4 km, where the overpressure is rather close to fracture limit (effective stress is close to micro-cracking level). However, the sharp transition zone inside source rock is practically missed on the velocity scale. The reason for this is low porosity response on overpressure effect due to gas generation (*Meissner*, 1981; *Gangi, Berg*, 1997), when highly compressible free gas compensates undercompaction effect on porosity scale.

It is important to point out that the application of any trend based Porosity Tool to this particularly frequent case could lead to quite big overestimation of the overpressure effect due to existence of significant non-homogeneity along the section (Base Cretaceous unconformity, lithology variation, etc.). Indeed, the real value of velocity departure from normal compaction velocity trend (the black marked curve in Fig. 11d) looks rather smaller then its possible evaluation based on extrapolation of a single trend line from Tertiary part down to Jurassic part. Searching for an unloading trend in agreement with Bower's method seems to be hazard operation without proven offset data in such depth. On the other hand, the hydrostatic – overpressure transition zone could be missed if it is caused by the gas generating source rock.

4.2.2. The Gulf of Mexico example

The formation setting illustrated in Fig. 10b was taken as a classical example of good conditions for ODVR application to overpressure estimation and prediction. Besides, historically it was the Gulf of Mexico basin where the very first positive experience in this challenge was achieved (*Pennebaker*, 1968).

It is generally accepted that the main overpressuring mechanism in the young and actively burying sedimentary basins like the Gulf of Mexico is non-equilibrium mudrock compaction (*Magara*, 1978). Continuous subsidence of the Earl Cretaceous "bottom" compensated by immense volume of clastic sediments via the antecedent Mississippi – Missouri river system creates appropriate environment for implementation of Terzaghi's one-axial effective stress model (6*) for description of a sediment rock compaction phenomenon (*Terzaghi, Peck*, 1948). This in turn allows reduction of challenge associated with the seismically derived overpressure prediction, because of rather close agreement between Earth model assumption and empirical data fitting methods. The deepwater conditions, however, look less favourable for these methods, since the top of overpressure normally coincides with the sea bottom here. It obviously prevents from establishing the normal compaction trend line position and, hence, from detecting the departure from it (*Dutta*, 2002a).

In addition there is one more important mechanism affecting the present day overpressure regime and violating assumptions of the background 1-D effective stress model (6*). This is salt tectonics, which violates with one-axial compaction model (10) and stress field model (6*). This violation increases during seaward rising and lateral progradation of salt diapir body (*Ge et al*., 1997). The analysis of basin scale subsurface salt movement on present day stress environment and the relevant anomaly in host rock compaction is far beyond the discussing topics. At this particular simulation example it is important to stress that the salt tectonic is an important additional factor violating the compaction – stress evolution model, which is essentially out of the background empirical models for any of Porosity Tools' based methods of pore pressure estimation. The salt tectonics' controlled mini-basin in the Gulf of Mexico offshore zone was chosen as an example for ODVR simulation. This case represents a didactic example of possible disagreement between simplified 1-D background stress model and real situation, which unavoidably misleads the relevant velocity data interpretation.

The formation section through calibration wells W1-W6 is reproduced in Fig. 12b-c in correspondence with the formation setting given in Fig. 10b. The central element here is a domal anticline created by young salt diapir, which folds and partially thrusts the enclosing part of the clastic Miocene formations.

The density log data observed in calibration wells located at the crest (W2) and at the flank (W3) parts of the dome reveal unexpectedly lower porosity level at shallower altitude of the same formation units (see Fig. 12a). At the same time excess hydrostatic pore pressure gradient was detected to be higher at the preaxial part of salt dome than at the flank parts (see Fig. 12b).

The paleo reconstruction of the salt seaward movement was based on backstripping analysis (*Rowan*, 1993). In particular, it indicates significant positive (thickening) and negative (thinning) thickness increment detected for evaporite and for cover part of the section, respectively, at the crest dome zone and reverse situation at the flank dome zones. This process appears to be most active during last two episodes of burial history (see Fig. 12c-e), when uprising salt diapir has got maximum buoyancy potential due to fast subsidence of the clastic section bottom.

Further calibration of compaction constants reveals clear visible positive anomaly in compaction associated with pre-axial part of the dome (Fig. 12c). This hyper compaction phenomenon detected above the front diapir edge section before its brittle deforming gives a good explanation of observed overcomaction effect

tracked in density – porosity signature (Fig. 12a). Moreover, the backstripping picture of burial history fitted to the thickness-porosity-overpressure data allows gross quantitative estimation of this effect in terms of additional increments to the vertical stress components associated with salt uprising and plastic deformation of the cover formations in the apex part (see Appendix for more details). The time distribution of additional to the effective stress components of salt driven pre-axial compression is represented in Fig. 12d.

Now, the synthetic porosity and effective stress curves obtained for the calibrated wells W2 and W3 in context of the described above local basin model allow simulation of ODVR through the section. The results of velocity simulations for the flank part (calibration well 2) and for the crest part (calibration well 3) are displayed in Fig. 13. The required for simulation parameters are listed in Table 1.

In contrast to the previous North Sea example, this case gives much higher estimation of expected velocity anomaly especially for the flank part, where the basin model does not contradict significantly to the background compaction model. The 5-6 % magnitude level for $\lambda(\xi_i; z)$ curve is getting observable from the depth 2.2 km and increases in the shale part of the section down to the 4 km depth where it reaches 10 %. The sandstone intervals in $\lambda(\xi_i; z)$ curve reveal less sensitivity to approximately the same level of target phenomena. The ODVR anomaly below 4 km sharply decreases.

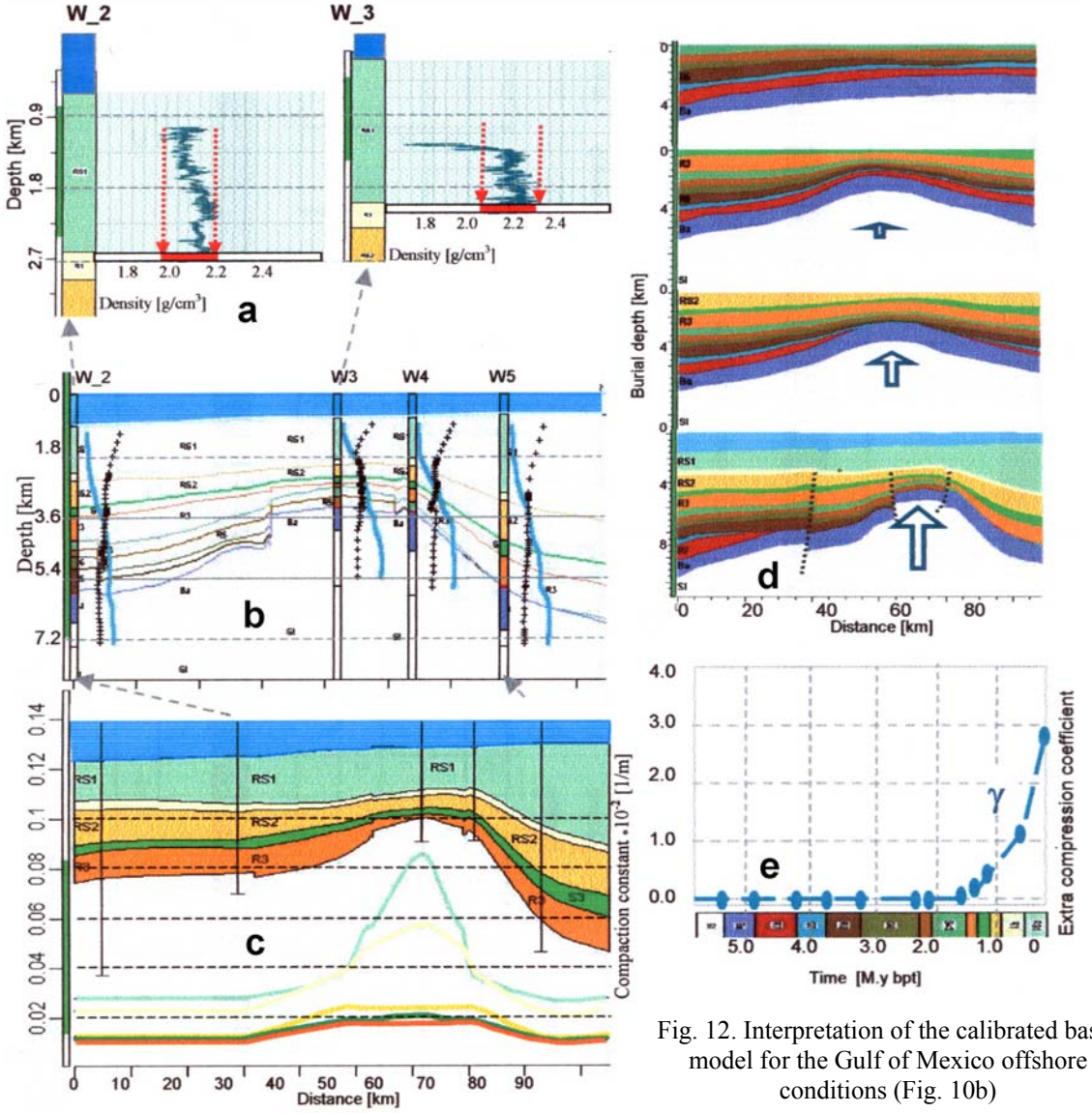

Fig. 12. Interpretation of the calibrated basin model for the Gulf of Mexico offshore conditions (Fig. 10b)

a – density log interpretation for flank and crest wells (the range of density variation is highlighted);
b – present day models of porosity and pore pressure fitted to the relevant data given along the section through calibration wells;
c – profile of calibrated compaction constants given along full section through calibration wells;
d – paleo reconstruction of the present day section (b,c) based on interpolating between backstripping results achieved for calibration wells during data fitting;
e – paleo reconstruction of effective stress environment in near crest locality in connection to seaward propagation of salt diapir.

The velocity response on overpressure at the pre-axial dome part looks less contrast. Furthermore, the normal compaction trend established for well W2 appears to be underestimating the expected level of porosity losses according to the basin modelling at salt involved compaction conditions. Thus, Porosity Tools' based pore pressure estimation could definitely give failure result in the apex part of this section.

The 3-D pressure communication phenomenon (centroid effect) (*Traugott*, 1996) for good permeable intervals (aquifer formations) can be considered here in addition to the salt induced hypercompaction effect. Indeed, sharply dipping aquifers potentially work as a lateral excess pressure equaliser. The centroid contribution into the overpressure effect cannot be estimated within the range of the simplified one-axial stress model and hence it is entirely out of the potential Porosity Tools' targets. The direct impact of centroid effect on velocity response in sandstones can possibly be detected if it rises the overpressure magnitude inside of the aquifer matrix up to micro-crack opening level.

Whatever effects contributing into the present day overpressure anomaly occur they could easily be missed and/or misled in the relevant velocity analysis, if they are out of the background Earth model.

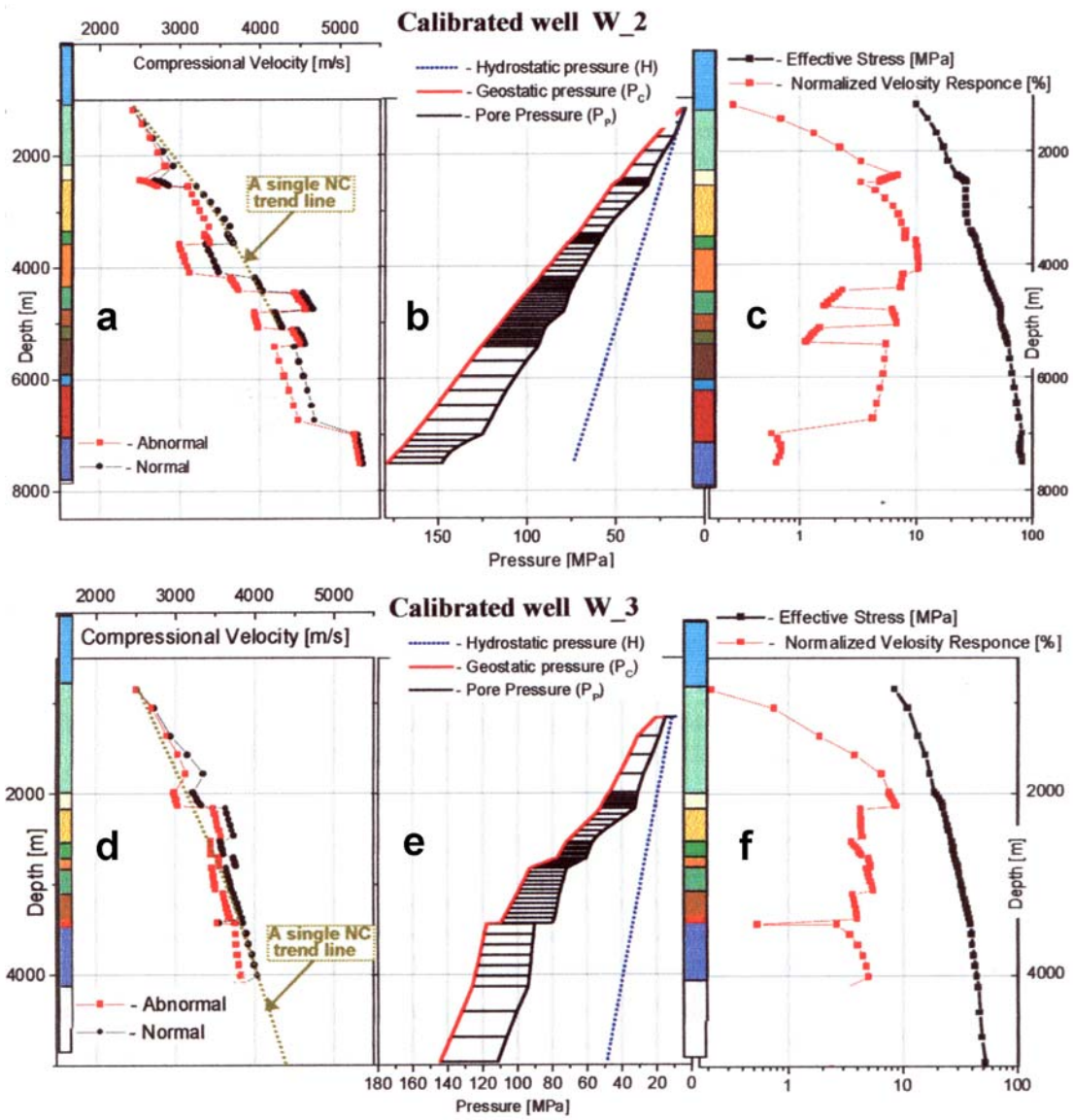

Fig. 13. The ODVR simulation based on calibrated basin model
for the Gulf of Mexico offshore conditions (see Fig. 10b and Fig. 12).

a,d – velocity model based on synthetic porosity and using Raiga-Clemenceau's equation for flank well (W2) and crest well (W3), respectively. The dark yellow dotted curve indicates position of the clay normal compaction velocity trend based on flank well (W2) porosity data fit;

b,e – the geostatic (P_c), hydrostatic (H) and actual pore pressure (P_P) curves based on the calibrated basin model (see Fig. 12) for flank well (W2) and crest well (W3), respectively (the differential pressure is stripped);

c,f – normalised velocity response (λ) vs. Effective stress (P_E) curves expressed in common logarithmic scale for flank well (W2) and crest well (W3), respectively.

4.3. Discussion

The seismic velocity response on the same target overpressure anomaly differs not only from sand to clay lithology, but also from shallow to deep part of the homogeneous (single lithology) section. In both lithology cases the ODVR is associated with departure of seismic velocity curve from trend position corresponding to normally compacted part of the section. This kind of depth velocity anomaly supposed to be interpretable as a response on transition from hydrostatic toward excess hydrostatic (overpressure) regimes of pore pressure. Note that reversing in velocity magnitude back from abnormally low to normal level with the depth is not possible, since stress and porosity losses are irreversible phenomena (*Magara*, 1978). Thus, detecting of the relevant reversal transition zone in pore pressure (from excess hydrostatic back to hydrostatic) by using any porosity – velocity tool is generally impossible.

As to the quality of the direct transition zone detection it is important to note the following.

According to the simulations in idealised homogeneous conditions the maximum sensitivity in ODVR is expected to be at the depth interval about 750-1000 m and 1000-1500 m for sandstones and mudrock, respectively. Here the relative velocity anomaly $\lambda(\xi_i; z)$ is comparable with realistic data error measure. Let the accuracy of seismic velocity estimation be 5 %. This threshold could potentially be exceeded within this upper sensitivity depth interval at low overpressure anomaly ($\xi \sim 1.35$ g/cm^3) for mudrock and moderate overpressure anomaly ($\xi \sim 1.5$ g/cm^3) for sandstone sections on condition that the background stress model is adequate and Porosity Tool is workable.

However, except of young rapidly subsiding region like the Gulf of Mexico or Nigeria basins, the overpressure occurrence, which potentially could generate drilling problems are normally detecting from below 2.5-3 km (*Mouchet, Mitchell*, 1989). Unfortunately, the velocity response to such occurrences becomes close and weaker that practically reachable data accuracy.

The simulation of ODVR for more representative and practically important Earth models can be based on real case analysis, basin modelling and calibration.

In particular, it allows prior estimations of the expected velocity anomaly for the section with mixed lithology and stratigraphy unconformity, where single normal compaction trend cannot be treated any more as appropriate for purposes' model. Besides of this, the more fundamental disagreement of real geology setting with background 1-D compaction $\leftrightarrow$ one-axial stress model could be checked and partially accounted for. This kind of simulation based on calibrated basin model has a big potential for correction of the background Earth model, apart from anomaly level control. This application will be considered below in connection with the real data examples.

5. Extraction of Overpressure Derived Velocity Response (ODVR) from seismic data

The multi-channel surface and well seismic data are the standard input for velocity analysis. In context of this section it is important to keep distinguishing between seismic velocity introduced above as target rock properties in connection with relevantly conditioned velocity model established for further interpretation (*Gardner et al.*, 1974; *Averbukh*, 1982; *Dutta*, 2002b) and seismic field velocity as a parameter of reflection wave field processing aimed for maximisation of some "signal/nose" ratio (*Dix*, 1955; *Urupov, Levin*, 1985; *Gelchinsky*, 1988; *Grechka et al.*, 1999).

It is commonly agreed that the seismic field velocity extracted from well seismic data (VSP, SWD, etc.) can be treated as a closet estimation of the relevant rock property suitable, in particular, for conversion into pressure scale and detection of the possible overpressure zone. Indeed, the seismic reflection field observed inside of a well is free from the apparent noise induced by surface seismic observations: multiples; low-pass filtering within the upper part of the section; processing induced errors: aperture and channels for stacking (for all Dix's model driven velocities); band-pass filtering; "signal/nose" framework model (for all inversion driven velocities).

Still the main advantage of using seismic data for pre-drill pore pressure prediction is associated with the frontier or completely virgin exploration areas with no well available in the target vicinity. Thus, VSP derived velocity anomaly detected in a well, which penetrates overpressure transition zone can serve just for accuracy control of "seismic field velocity $\rightarrow$ pore pressure" conversion, whereas the surface seismic data remains to be the most attractive data source for pre-drill overpressure prediction.

There is a variety of techniques aimed for extraction of seismic rock velocity from surface seismic data. The different kind of stacking velocity analysis represents the first group of techniques aimed for perfecting the seismically driven 3-D image of subsurface. Generally, any of interval seismic velocity estimations based on conventional stacking data analysis (RMS, CMP, DMO, CRP, CRE velocity analysis, etc.) are not purposely oriented kinematical characteristics of wave field, despite that they could be often misused for overpressure prediction. Now it is commonly agreed that no one from such interval velocity parameters can be suggested for the purposes of overpressure estimation and/or prediction because of low spatial frequency, high dispersion of results and excess of its absolute values from real rock property (*Al-Chalabi*, 1994; *Dutta*, 2002a). The different seismic data inversion techniques (*Bleistein et al.*, 2001) potentially can provide higher resolution and more consistent with in situ (VSP) and lab measurement results, which supposed to be suitable for purposes (*Sayers, Johnston*, 2000; *Sayers et al*., 2002; *Dutta*, 2002b; *Huffman*, 2002; *Lopez et al*., 2004).

5.1. Brief review of appropriate approaches

As it was stated above, this paper is not aimed for analysis of seismic data inversion techniques and suggestions of the best one for the purpose. We address readers to the recent review published by N. Dutta in Geophysics issue (*Dutta*, 2002b).

Here we just briefly describe three most popular in our context seismic data inversion approaches and summarise their inherent restrictions in order to confront them with inherent forward model limitations discovered above for target ODVR.

The seismic data inversion tools commonly used for extraction of rock velocity could be listed according to the complexity of background velocity models as the following:

1. Tomography and prestack depth migration.
2. Velocity based on 2-D/3-D AVO response inverting.
3. Velocity based on full-waveform inversion.

A Reflection Tomography approach (*Sayers, Johnston*, 2000; *Sayers et al.*, 2002) substitutes low resolution, the simplified media model and relevant hyperbolic move-out assumptions implemented for stacking velocity methods with more general and flexible ray-trace modelling based approach. Essentially, this approach implies inversion into the 3-D velocity model with changeable along the depth and arbitrary oriented reflectors (*Goldin*, 1986). The iterative process of the model fitting converges to the prestack depth migration maps where CIP reflectors have the maximum contrast and resolution.

Note that this approach is purposed on perfecting some 3-D seismic image of subsurface. Thus, its application to the overpressure analysis can be treated as one of incidental product.

A 2-D AVO response inverting approach (*Bach et al*., 2000) is based on approximation of natural reflector by the set of thin transversely isotropic layers stacked between two half space and inverting of restored amplitude versus offset variation into the relevant reflectivity model with respect to Young's modulus (*Matlick*, 1995). At this, a requisite offset geometry for particular subsurface target should be predefined in the form of low-frequency velocity trend and the density information assumed to be accessible or available (for example, from Gardners' approximation (*Gardner et al.*, 1974)).

Note again that this approach was initially aimed for identification of thin layered impedance model for target exploration intervals (*Castagna, Backus*, 1993). Since that time the background sandwiched model of media was not changed in a way to accommodate the target phenomenon features such as local stress variations, undercompaction or free gas generation within the pore space. Thus, the background rock physics model as a start point of data inversion is far from appropriate for purposes.

A Full-waveform (FWF) Inversion approach (*Dutta et al*., 1998; *Dutta*, 2002b; *DeKok et al*., 2001) suggests using large offset conventional *P*-wave data and constraining of possible inverse problem solutions with appropriate rock physics models. At that, input data for inverting includes full scale angle gathered records of high resolution prestack seismic data. The inverting strategy implies minimising of misfit between synthetic and real wave field within the work time gate (*Charara et al.*, 2000). Synthetic seismograms are based on exact wave equation solution constrained from low-frequency density-velocity trend model and reasonable assumptions about rock mechanics and fluid dynamics in the area of investigation. All interference and transmission effects due to thin layering and velocity gradients assumed to be accurately accounted in forward problem solution. Statistical optimisation (if it is involving into misfit minimising) delivers some measure of the uncertainty at the elastic modulus' estimation within the range of the predefined rock physics model.

The background rock physics model associated with this approach looks most general and suitable for accommodation of the necessary model parameters sensitive to manifestation of the target phenomenon.

On the other hand, this model obviously is most complicated by definition. Thus, the relevant seismic data inversion technique is expected to be the most uncertain, non-stable and time consuming operation.

There are several important points to be taken into account when talking about extraction of target rock velocity response from surface seismic data by using this approach.

Implicit forward velocity model errors. The background rock physics model in full-waveform Inversion approach must contain too much hidden parameters that affect implicitly the velocity value apart from target overpressure phenomenon in order to be full enough. For example: inherent earth property like anisotropy, lithology changes, inherent pore fluid phase content changes; geometry variation from horizontal layering. In addition it should exclude or account as a noise component of the model all processing and observation factors mentioned above. Clear, that any of these factors being ignored in the forward velocity model will form apparent noise and will contribute to non-unique inverse problem solutions in the form of implicit forward model errors.

Computer limitations. The full-waveform Inversion approach is based on complete solution of the elasto-dynamic wave equation, which requires a computational power that is several orders of magnitudes higher than that of traditional processing methods. This makes complete and realistic solutions of 3-D problems

unfeasible, even with today's supercomputers. The present day full-waveform inversion algorithms are mostly addressed to 1-D and 2-D inverse problems (*Al-Dajani et al.*, 1999).

Uncertainty and non-uniqueness of data inverting. The full-waveform Inversion is non-linear and severely ill-conditioned math problem posed for vast dimensional model parameter space. These difficulties combine to treat it as a very complicated mathematical exercise generally addressed to optimisation techniques.

Whatever class of the velocity model is taken as a background model: deterministic or stochastic, the least squares or most like solution of the relevant inverse problem posed for surface seismic data only, exhibits large uncertainties and non-uniqueness because of the ill-conditioning (see, for example, *Tikhonov, Arsenin*, 1979; *Tarantola*, 1987). This means that generally there is a continuous set of Earth models which are fitted the observed data within an error comparable with an acceptable noise level. All these models are candidate solutions to the inverse problem.

Whatever search strategy is implemented for the full-waveform Inversion, it is necessary to reduce as much as possible the dimension of model attribute space and to have a good starting point inside of it in order to obtain a rapid and conditionally unique convergence. The non-linearity of this inverse problem is most severe for low wave-number perturbations of the velocity model. Therefore, the initial model should be approximately correct in the low wave numbers.

Thus, the common disagreement between requirements to the seismically derived overpressure prediction approach and success of seismic data inversion is need in getting *a priori* information and calibration wells within the frontier prediction areas.

5.2. Real data examples

There are three examples presented here to illustrate real case interpretation of velocity anomaly vs. proven overpressure anomaly. They belong to three different sedimentary basins with rather different geology settings and regional overpressure origins. The first one is the Jeanne D'Ark basin within the continental margin of eastern Canada with complicated and mosaic overpressure signature at the target Base-Cretaceous – Upper Jurassic level. The second one is the Petchora Sea basin with the laterally consistent overpressuring within the Paleozoic carbonate section. The third one belongs to the north onshore part of the huge Western Siberia sedimentary basin with well consistent continuous clastic section and regularly detected pore pressure problems attached to the late Jurassic formation level.

The stratigraphy-lithology settings for all three cases study examples are represented jointly in Fig. 14.

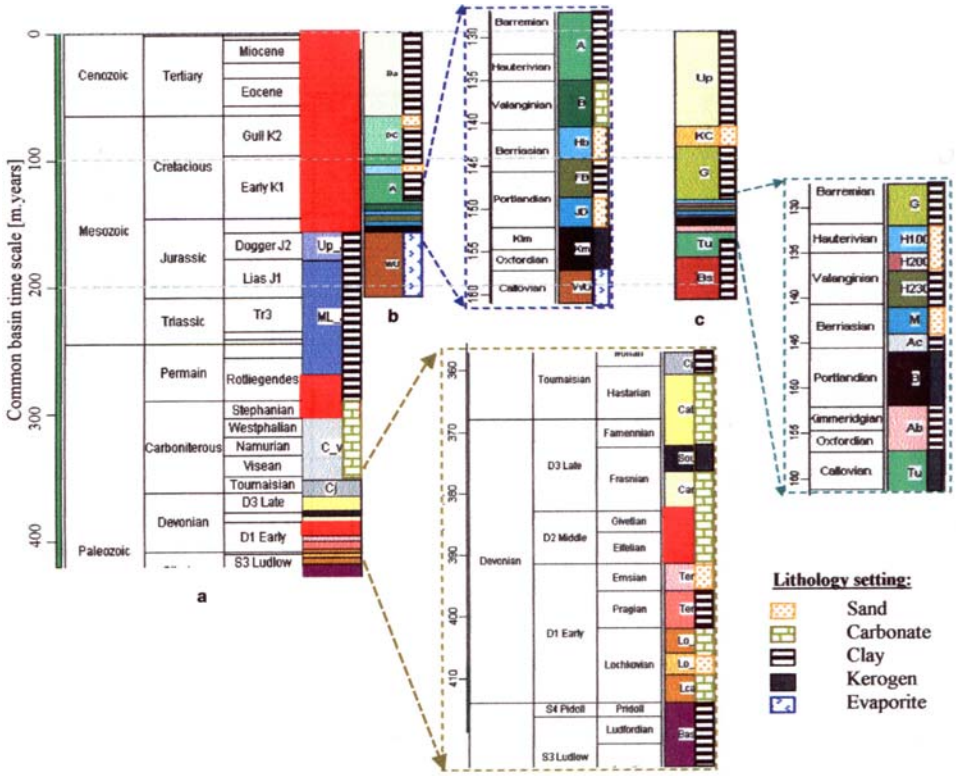

Fig. 14. The local stratigraphy columns for calibrated areas used for ODVR real case analysis.
a – Petchora Sea basin, Varandey-Adzvinsky region (the locally eroded formation highlighted with the red colour);
b – Eastern Canadian offshore, Jeanne D'Ark basin;
c – North-Western Siberia onshore.

The Jeanne D'Ark example illustrates applicability of surface seismic data for production of spatially vast overpressure estimations (pore pressure cube). Both Petchora Sea and Western Siberia examples are based on VSP derived seismic velocity that was considered above as the closest to the rock velocity estimation accessible form seismic data in a well. Thus, they can impartially illustrate lithology-stratigraphy control on in situ ODVR and also demonstrate accuracy of conventional seismic rock velocity → pore pressure routine (see Fig. 7).

5.2.1. The surface data example from eastern Canadian offshore

The Jeanne D'Ark basin belongs to northeast – southwest oriented basin system of Grand Banks related to the Appalachian orogen. The general geology-tectonics information is widely published (see, for example, *Grant et al.*, 1986; *McAlpine*, 1990). The present day image of Cenozoic – Mesozoic section could be associated with considered above the North Sea graben with the thick (up to 4000 m in the centre part) Tertiary clastic deposits, mixed deltaic and shallow marine clastics target intervals in the Upper Jurassic sub-section and even with major unconformity related to the latest Jurassic – Early Cretaceous uplift and erosion. Still the much sharper lateral variation in litho-stratigraphy and presence of active salt tectonics make the geology setting here more complicated.

Here overpressure phenomena were detected and analysed mainly in Jurassic formations. The stratigraphy and magnitude levels of the top transition zone vary sharply from south to north part where they are youngest and highest, respectively.

According to overpressure origins' investigation (*Mudford*, 1988; 1990) and our own basin model calibration results the present day 3-D overpressure picture could be interpreted as a cumulative result of several pressure retaining and pressure generation mechanisms acting simultaneously, which could be listed as the following:

1. Poor pressure communication of overpressured Late-Middle Jurassic formations with the remote pressure discharge zone (hydrostatic regimes) through the series of across-basin faults, which form lateral pressure barriers.
2. Tough shales within the upper Jurassic interval (formation "FB" and "B") and massive mudstones of Early Cretaceous (formation "A") in combining with the above mentioned mechanism additionally embarrass pore fluid releasing during sedimentary rock compaction within the areas where the Base Cretaceous uplift – erosion episodes were short.
3. HC generation from matured Jurassic source rock (formation "Km") on temperature-pressure conditions where gaseous phase can be freely injected into pore space.

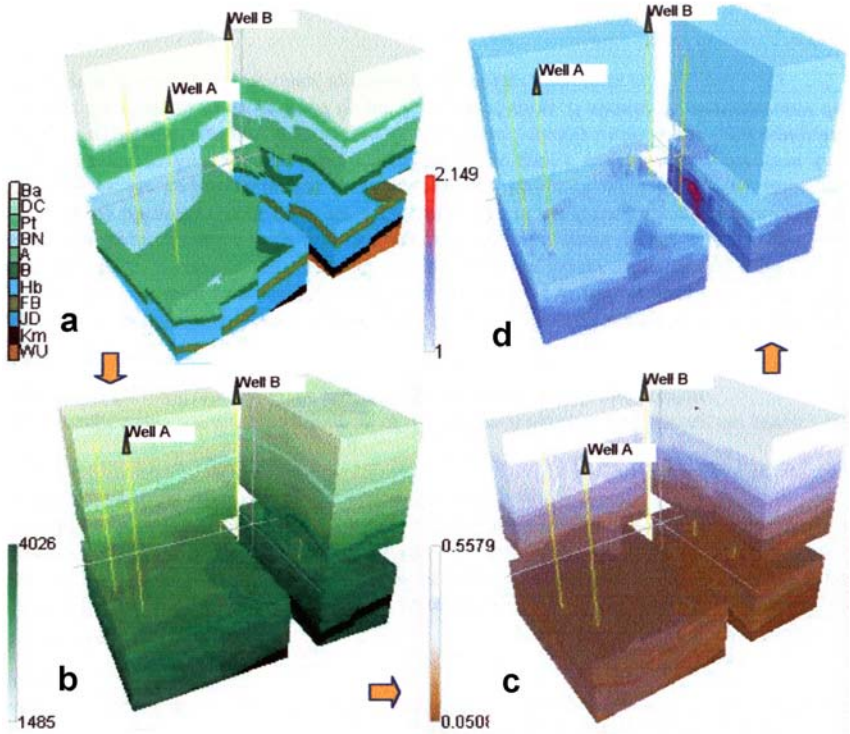

Fig. 15. The 3-D estimation of overpressure in the Jeanne D'Ark basin based on standard data cube conversion: velocity → porosity → overpressure (see scheme in Fig. 7).

a – formation cube for depth interval 500-5000 m (the geometry image is given in scale proportion X = 1; Y = 1; Z = 10);
b – seismic interval velocity cube. The velocity scale gives Min – Max variation in m/s;
c – porosity cube based on cube (b) transformation. The porosity scale gives Min – Max variation in fractions;
d – overpressure cube based on cube (c) transformation. The pressure gradient scale gives Min – Max variation in g/cm^3.

The attempt to predict overpressure from surface seismic data in the form of conventional pore pressure cube converted from interval velocity cube is illustrated in Fig. 15 and 16.

The 3-D seismic data were processed in the way to get purposely conditioned interval velocity estimations. The results were interpolated on the regular 3-D grid in the form of velocity cube (see "velocity cube" in Fig. 15b) and then approximated formation-by-formation in agreement with the Earth model (see "formation cube" in Fig. 15a) in order to extract and estimate trend component of the relevant "velocity macro model" (*Traugott*, 2000; *Madatov, Sereda*, 2000b). The high frequency interval component and low frequency trend components of the seismic field velocity were then mixed in the way to provide the best fit with the source seismic TWT data. Further transformation of "velocity cube" (Fig. 15b) into "porosity cube" (Fig. 15c) and "pore pressure cube" (Fig. 15d) were made in correspondence with the work flow scheme displayed in Fig. 7.

The quality of predicted pore pressure was controlled on several calibration wells by comparison of velocity derived conventional pore pressure curves extracted according to the relevant coordinates from the output cube (Fig. 15d) against available pressure data and synthetic pressure curves fitted to these data (see block 3 of generic work flow scheme in Fig. 9). The comparison results for two wells named "A" and "B" in Fig. 15 are represented in Fig. 16 jointly with gamma ray logs, indicating lithology variations along well trajectories.

The velocity derived conventional overpressure 3-D picture in general and for the control wells, in particular, reveals significant underestimation of magnitudes and lack of contrast in reproducing most like positions of transition zones. Apart from inherent low resolution of surface seismic data this could be due to low flexibility of the background trend velocity model as a common disadvantage of any Porosity Tools.

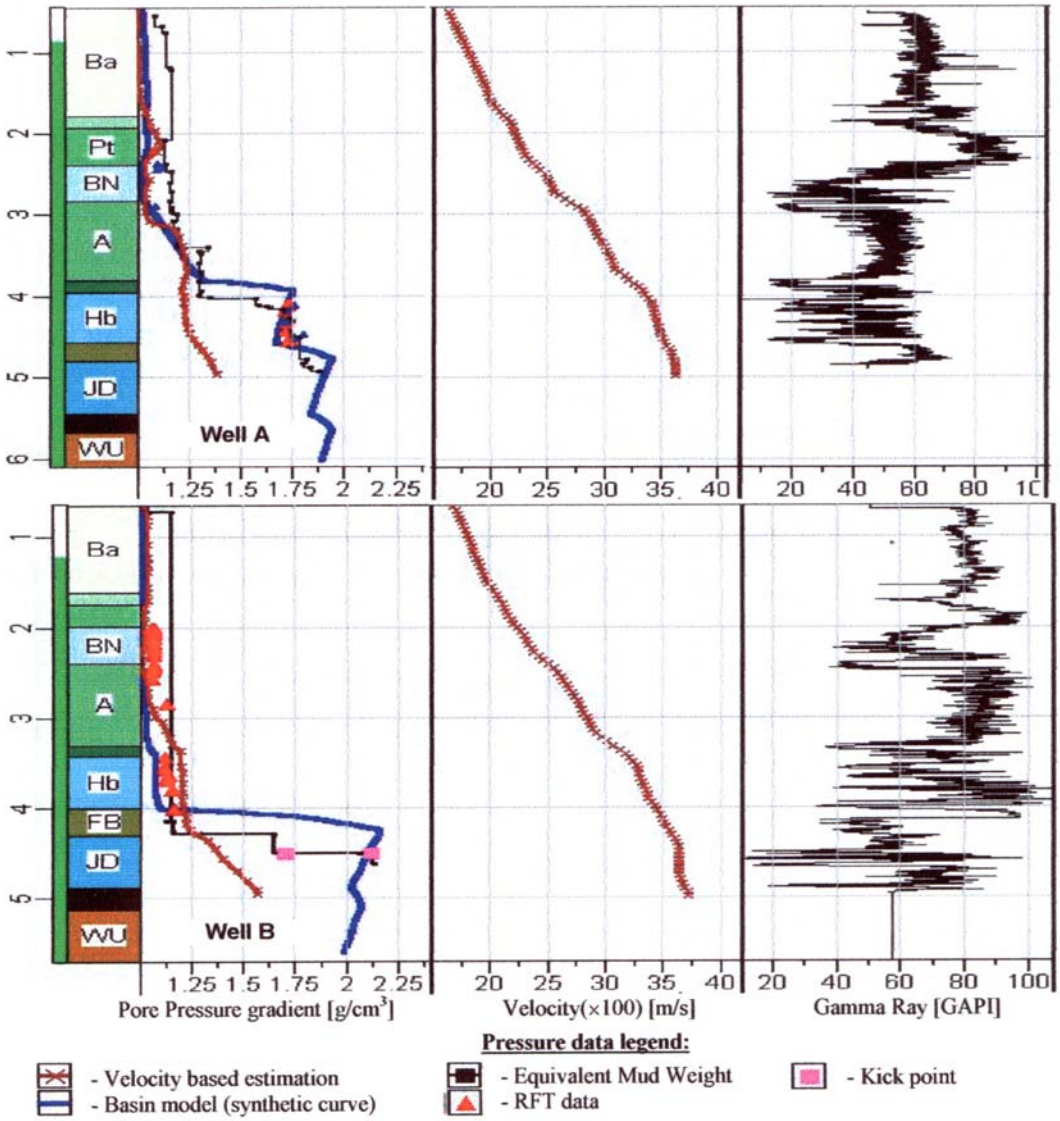

Fig. 16. The Jeanne D'Ark basin area. Overpressure estimations based on velocity data cube vs. calibrated basin model and other direct and indirect assessments for two calibration wells in the area (see also Fig. 15)

5.2.2. The VSP data example from the Petchora Sea

The area of this real case sample belongs to the Varanday-Adzvinsokaja zone of the Timano-Petchorskaja oil province described in the published literature (see, for example, *Solomatin et al*., 1988; *Botieva, Shoulova*, 1991; *Zagoulova et al.*, 1994). In contrast to all the reviewed in this paper geology settings, this is a typical representative of an old carbonate section with vast eroded intervals and severely changed diagenetically exploration targets (see Fig. 14a). In particular, the Devonian clastic and carbonate reservoirs (formation units "Te_1", "Lo_2") and clay-carbonate source rocks (formation unit "Sou") are sandwiched here by pretty well compacted shale and carbonate formations within the depth interval about 3.0-4.0 km.

The indirect overpressure drilling attributes and few direct RFT measurements indicate existing of the regionally stable overpressure zone in close proximity of exploration targets with rather sharp transition zone (see Fig. 17).

The origins of overpressuring in the area are poorly understood as well as the empirical links between velocity and porosity in compacted shale-carbonate rocks are not established.

The interval velocity profile derived from detailed VSP data analysis reveals good correlation with lithology changes along the depth axis according to the core and well logs analysis (see Fig. 17). In particular, well-compacted carbonate parts of the section (formation "Cab") are clearly detected on the velocity scale. The reversing in low frequency velocity trend back to moderated magnitude below carbonate bottom is also in agreement with lithology changes (see Fig. 14a). Perhaps the departure from the normal trend could be detectable in agreement with the sharp transition zone between formation units "Te_1" and "Lo_2" if its "normal" position were recoverable from additional sources of information. As it is clear from the velocity plot in Fig. 17, the extrapolating of a single Raiga-Clemenceau's trend fitted to the data in the upper part of the section (Middle-Early Jurassic mudrocks) does not allow detecting of the expected departure in velocity values. Formally, the target part of the section appears to be overcompacted, that probably is the case from pure mechanical point of view. One way or another, the proven overpressure zone below formation units "Te_1" remains to be formally hidden in velocity response.

To all litho-stratigraphy appearances the secondary porosity losses and overpressure generation mechanisms are dominating in this interval of the section. Evidently, that the background stress-porosity-velocity model is too simple and not adequate for purposes in similar conditions.

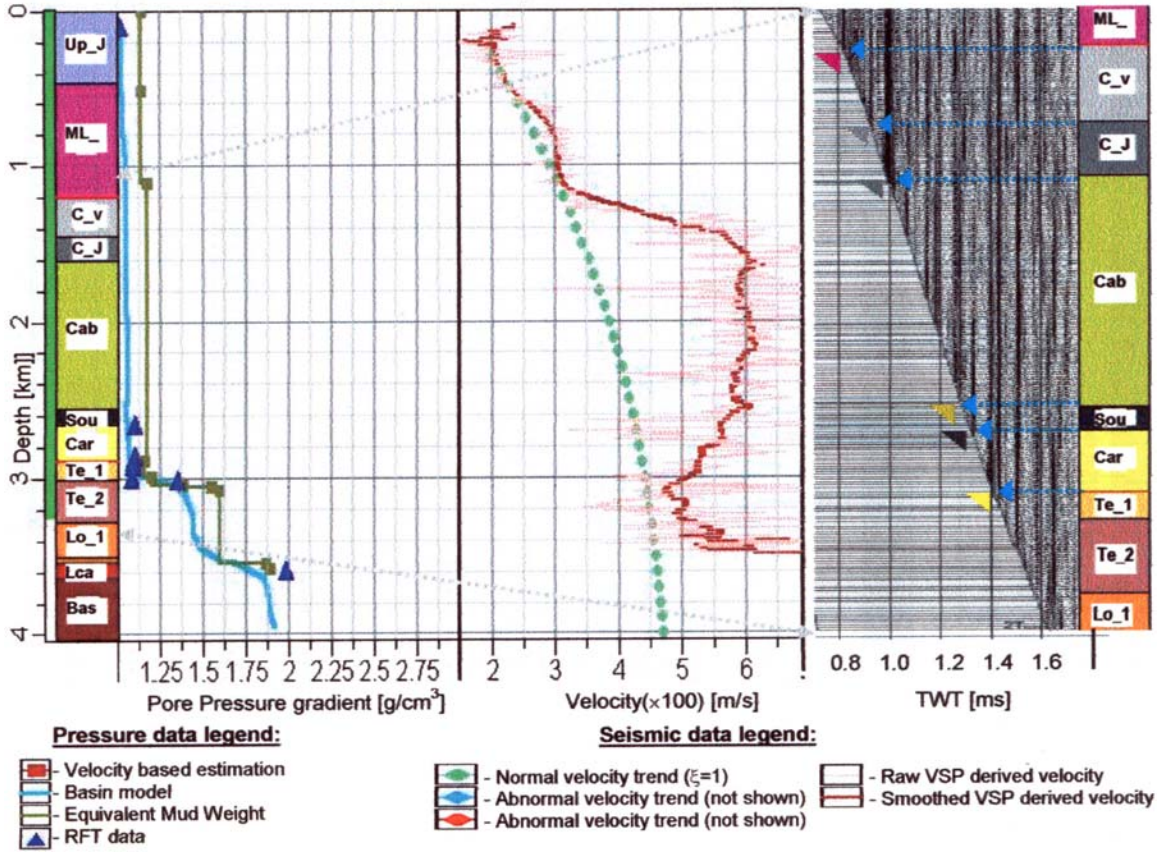

Fig. 17. The Varandey-Adzvinsokaja region of the Petchora Sea basin (see also Fig. 14). Overpressure estimations based on VSP derived velocity data. The massive carbonate interval (formation "Cab") is highlighted. The zoomed part of the section with the VSP data attached is marked by arrows.

5.2.3. The VSP data example from the North-West Siberia onshore

The West Siberia region is the worldwide largest continental sedimentary basin, which contains one-third of world gas reserves. Its geology settings and HC-migration – accumulation features are broadly described in Russian and international issues (see, for example, *Kontorovitch*, 1975; *Krouglikov et al.*, 1985; *Littke et al*., 1999). In particular, it is well known, that the greatest part of explored gas reserves (about 65 %) are here attached to the Cenomanian reservoirs at shallow depth (800-1200 m), where it is represented by almost pure methane in gaseous and partially dissolved phases. Still, the older and deeper parts of the section are also potentially oil and gas bearing and hence are representing a future exploration target.

The basin was originated mainly from Triassic continental rifting. Thus, its formation column is mainly related to Cenozoic-Mesozoic stratigraphy interval (see Fig. 14c). However, in contrast to the North Sea rift basins and East Canadian continental margins its burial and thermal history according to paleo reconstruction and basin modelling results (*Littke et al*., 1999) is assumed to be more continuous and regionally stable and its sediment fill is interpreted to be more homogeneously clastic. The vast transgressions were here gradually changed on regressions covering large areas. In particular, the vast marine transgression during Late Jurassic led to regional depositing of principal source rock in the region (formations "B" and "Tu" in Fig. 14c). The marine environment during Early Cretaceous was regionally changed on more continental one with deltaic progradation of clastic deposits associated with high sedimentation rate. This stratigraphy interval is almost everywhere correlated with presently regional gas reservoirs (formation "KC") supplied with secondary migrated gas by long distance groundwater flow from the south HC-generating areas (*Krouglikov et al.*, 1985). The largest sedimentation discontinuity in the area associated with late Eocene uplift occurrence when up to 500 m of a formation thickness was eroded.

The experiences in overpressuring and the relevant drilling problems in the region are typically related to attempts to explore deeper frontier intervals in the close proximity to the upper source rock level (formation "B"). The overpressuring phenomena within these older intervals of the section were estimated to be increasing from 1.25 up to 1.9 g/cm^3 in equivalent mud weight scale along interval of formations "H230-B" (typically: 3500-4000 m). Judging from the present day underground temperatures at this interval (110-130°C), which coincides with gas-cracking-generation windows for locally matured source rock (*Tissot, Welte*, 1978) the primary important overpressuring mechanism here could be related to recent or still continued primary gas generation (*Gangy, Berg*, 1997; *Littke et al*., 1999).

The set of deep exploration wells in the area was used for calibration of the overpressure purposed basin model (*Madatov, Sereda*, 2000b; 2003). The synthetic porosity and overpressure curves (see block 3 of the generic work flow scheme in Fig. 9) then were fitted to the available real data prototypes and used for continuous estimations of overpressure profile along the whole well paths. Some of the calibration wells were also seismically logged later and the VSP data were obtained from whole depth interval. The VSP data were used for geological identification of main seismic horizons in the area and for producing of high quality interval velocity analysis. The good consistency of results and its close correlation with lithology changes and gas log data gave us a chance to interpret this seismic velocity as a high quality estimation of seismic rock velocity suitable for target purposes. It allows in turn to use the final velocity profile for producing overpressure estimation according to standard routine (see Fig. 7) and then to compare it with the basin model derived overpressure estimations against post drill overpressure estimations. In particular, the sensitivity and stability of ODVR regarded to perturbations of tuneable parameters of background velocity $\rightarrow$ pore pressure conversion model implemented in standard routine were investigated. The results are represented in Fig. 18 and 19.

The velocity plots include raw and smoothed interval velocity estimations derived from VSP data analysis jointly with Raiga-Clemenceau's trends produced for fixed undercompaction – overpressuring levels. Note, that the normal rock velocity trend was fitted to the upper part of the relevant velocity data attached to mudrock parts of the section, where clays assumed to be normally compacted with no overpressure indications. An acceptable match to velocity and porosity data allows fixing of necessary parameters in the relevant empirical relationships (see formula (15)) and using them for production of theoretical transparency. Landro's formula (9) was used to calibrate velocity $\rightarrow$ pore pressure conversion model for sandstones against saturation (ΔS) and overpressure (ΔP) data available at the Cenomanian reservoir level (formation "KC"). The relevant velocity trends are not shown.

The data control tests reveal rather good accuracy in the detection of the upper transition zone from hydrostatic to excess hydrostatic pore pressure level consistently detected just below formation H200 (highlighted strip in Fig. 18). At the same time the formal implementation of standard velocity $\rightarrow$ pore pressure conversion model through all the section intervals did mislead to an artefact low-to-moderate overpressuring anomaly through all the Cretaceous intervals which is neither consistent with the overpressure indications nor with pressure simulation by basin modelling. On the other hand, the "departure form normal compaction velocity trend" regularly detectable at the Cenomanian reservoir level (formation "KC") most likely indicates nothing else but well proved presence of gas phase inside of pore space within the relevant gas field interval. Both phenomena produce a negative anomaly in rock velocity for sandstone (see Fig. 3,4) and evidently cannot be interpreted separately within the Landro's empirical model unless one of the model parameter (saturation or overpressure) is given from outside *a priori*.

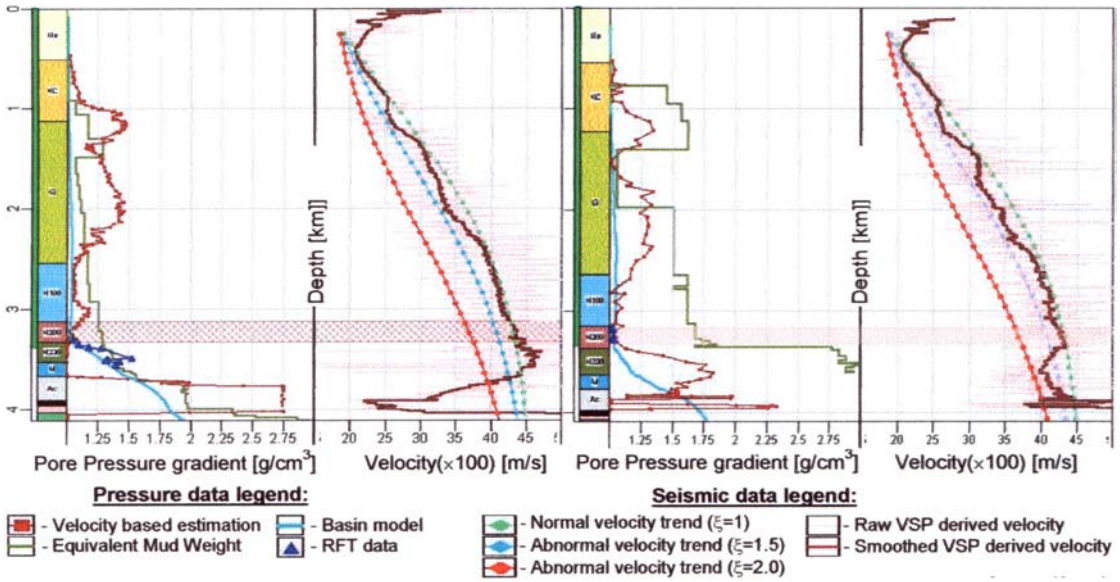

Fig. 18. North-Western Siberia onshore (see also Fig. 14) overpressure estimations in two neighbouring wells based on VSP derived velocity data

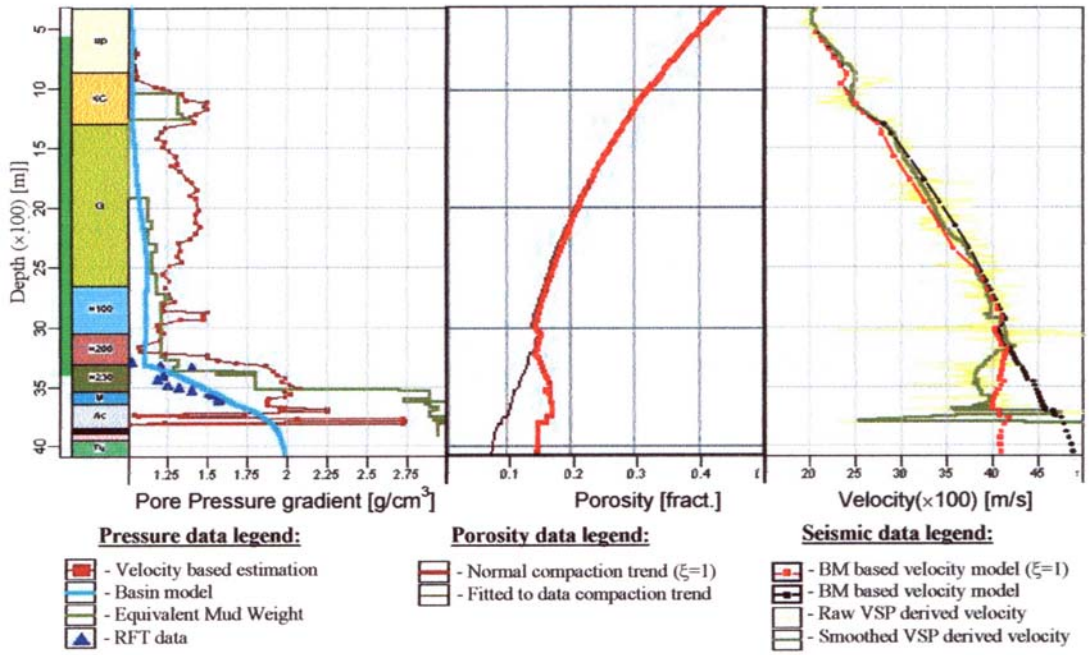

Fig. 19. North-Western Siberia onshore overpressure estimations based on VSP derived velocity versus the basin model of formation: overpressure (left), porosity (middle) and compressional velocity (right)

The ODVR level at the bottom part of the section does not behave stably. Indeed, the upper part of the departure anomaly gives generally acceptable fit with basin modelling and pressure data but below formation "M" the overpressure response varies too sharply and within totally unrealistic variation range. Apart from inherent non-stability of differential transformation applied to produce interval velocity estimation, the reason for this is a non-adequate earth mode implemented within the interval of well matured source and gas generating rocks (*Littke et al*., 1999). As it was stated above (see s/section 3.2) a source rock normally reveals a high level of anisotropy. The primary gas migration from Keorgen and corresponding overpressure generation could produce cumulative effect on rock velocity in the form of severe local decreasing of its magnitude up to 25-30 % of the relevant "normal" value (*Gregory*, 1976; *Domenico*, 1976). Thus, high quality velocity analysis ensured here in VSP derived data is not yet a guaranty of stable and accurate conversion into the pore pressure scale. It seems that in this case any single mechanism or *a priori* paramount factor laid in the background model can mislead explanation and interpretation and over/under estimate the target overpressure anomaly. This is especially true for deeper than 2.5-3 km exploration targets approaching to the underground temperature interval above 110°C.

5.3. Discussion

The stacking velocity analysis can formally provide transformation of the relevant 3-D interval velocity data cube into pore pressure scale. In other words, it ensures building up of the corresponding pore pressure cube at reasonably short time and price. At all appeal of such a quick and massive output its accuracy and practical value remains to be questionable. Moreover, the target results with the big probability can be missed in final transformation due to: objective restrictions of the relevant processing; oversimplified velocity → pore pressure conversion model and generally weak sensitivity of rock velocity response to the target phenomenon at the depth level, where it normally becomes noticeable.

The VSP derived interval velocity profiles certainly reveal higher quality and correlation with the target. Thus, the objective limitations in surface seismic resolution plus artefact errors related to non-purposely oriented wave field processing are an important noise factor. Still the next two problems remain to be non solvable so far: low flexible and inadequate velocity → pore pressure conversion model and weak sensitivity of rock velocity response to the secondary processes' driven overpressure phenomena.

Unfortunately, decreasing of ODVR sensitivity with the depth cannot be controlled and fixed. All what can be done is an improvement of the background Earth model aimed for more flexible and extensive accommodation of all available and related to phenomena information, including geology, rock physics, basin analysis in addition to presumably main (but not last!) source – seismic data.

Let us consider this part closely.

It is commonly agreed, that the inversion of seismic data should be somehow constrained with the reasonable petrophysical model restrictions (*Tarantola*, 1984; *Goldin*, 1986; *Dutta*, 2002b).

Depending on the class of a forward model established to describe a target phenomenon the searching strategy in full-waveform Inversion could vary from a global optimisation technique (mimic or stochastic models) to a local optimisation technique (a deterministic model) (*Menke*, 1984; *Bleistein et al.*, 2001).

Since *a priori* information about a target phenomenon is absent or cannot be accommodated into the background model and its proper upscaling is missed the conventional and robust strategy remains to be global optimisation represented, for example, by a generic algorithm (*Goldberg*, 1989) or a simulating annealing algorithm (*Goffe et al.*, 1994). Despite of hard computing it provides generally acceptable solution, which could have practical sense when reasonable model constrains can be attributed.

The alternative in the form of local optimisation technique can have sense as far as an attribute space of the background model is able to accommodate prior information in the form of reasonably compact sub-space on it and if such *a priori* information can be made available. In this case the classical local optimisation techniques (gradient or Newton-like methods) with soft and/or hard constraining provide stable and locally unique solution and requires less in orders computer time to reach it (*Menke*, 1984; *Tarantola*, 1984; 1987).

The question rises: can we improve the background for seismic data inversion model in the context of more adequate velocity → pore pressure conversion than it is commonly used up to now?

We believe that the reserve of improvements is not exhausted yet.

The idea of combining seismically derived empirical models with the deterministic basin scale model of pore pressure evolution is not new at the discussing topic (*Madatov et al.*, 1995; *Traugott*, 2000; *Düppenbecker et al.*, 2002). However the way of such combining remains to be uncertain for most of the practical applications.

Our own experience in the multi-source data inversion in regard to the basin scale pore pressure evolution model reveals big potential for extension of both the model attribute space specification and the type of sensitive to target data involved into the inversion process. Indeed, the pressure and porosity multi-well data inversion allow the calibration basin model parameters, which in turn controls important for velocity → pore pressure conversion attributes: compaction constants, HC-generation potential, etc. The main disadvantage of basin modelling approach to the target prediction problem is associated with needs in calibration wells to be presented within the area. First of all, the same problem in not avoidable for seismic data inversion, unless it is based on a very general and, hence, very simple Earth model. Secondly, the macro-level (trend) model required for reconstruction of full component of the relevant rock velocity model assumed to be associated with the averaged along big depth interval (hundreds of meters) and slowly changeable laterally formation property like lithology controlled rock compaction or fluid conduction constants, which just are the output parameters of basin model calibration.

Thus, one of the simplest solutions in combining of background Earth model at well data and seismic data inversion could be the following.

The basin model driven trend model could be converted into velocity scale by using available empirical deterministic solutions and then it can serve as a proper start point for the next stage of inversion (full-waveform Inversion of seismic data) in context of the target prediction problem.

This approach is illustrated in Fig. 19, where the forward rock velocity model was computed based on considered in section 3 empirical relationships. Note that the real data example in Fig. 19 is fitted to the available VSP velocity data in the upper part. It was not possible to compensate the velocity data-model misfit in the abnormal part of

the well section just by tuning corresponding compaction constants, which were constrained by fit of synthetic porosity and synthetic pressure with the relevant real data. The free for tuning parameters in this case remains gas controlling attributes regulating HC generation in source rock (TOC, HI, etc.) and its secondary seaward migration (GOR, GWR, capillary break on pressure, etc.). It is important to stress that the more general and fundamental is the background Earth model, the more range stable and independent from area location its calibrated parameters will be.

6. Conclusion

A poro-elastic model describes rock velocity as a function of elastic modulus, bulk density and some microscopic properties of the media model like grain to grain contact and/or stiffness, pore volume changes, critical porosity and so on. The explicit dependence of rock velocity from pore pressure appears only for a high frequency Biot model to provide account for the relative solid – fluid pore scale motion during wavelet propagation. However, this pore pressure change belongs to specific high frequency phenomena and is not characteristic of prediction target – excess hydrostatic pore pressure. Besides, the high frequency Biot model is robust for ultrasonic data only.

The pure impact of target phenomena on seismic velocity (Overpressure Driven Velocity Response – ODVR) is not independent even for a homogeneous isotropic medium approximation but mixed with other macro and micro scale phenomena like changes in mineral content (lithology), HC saturation of pore fluid, anisotropy, etc.

According to lab investigations the rock velocity for well grained clastic rock matrix (sand/sandstone) reveals high sensitivity to the pore pressure changes at the low level of the differential pressure (15-30 Mpa), which corresponds to microcrack-closure stress level. This sensitivity to the target yet gradually decreases with the depth because the pore pressure increase is not completely cancelled with the relevant effective stress decrease anymore (*Prasad, Manghnani*, 1997). It is logically to connect the high sensitivity of ODVR to pore pressure changes with the zone where the excess of pore pressure over the hydrostatic level is close to fracturing limit, where the relevant rock-fluid system dramatically changes its elastic response (*Nur, Dvorkin*, 1998).

The clay/mudrock velocity response on pore pressure changes is less investigated in lab. The empirical basis for the relevant seismic velocity → pore pressure conversion is established on in situ relationships between velocity and porosity of these materials (*Hubbert, Rubey*, 1959; *Smith*, 1971; *Dutta*, 1983) and then on standard (*Magara*, 1978) or extended (*Bowers*, 1995; *Seberyakov et al.*, 1995) Porosity Tools used for bijective conversion of undercompaction estimations into overpressure anomaly.

The simulation of ODVR for speculative homogeneous Earth models allows to allocate and range the sensitivity areas within the coordinates plane "relative overpressure anomaly vs. relative velocity anomaly" for two different lithologies: sandstone and mudrock. In particular, the maximum sensitivity in ODVR is expected to be at the depth interval about 750-1000 m and 1000-1500 m for sandstones and mudrock, respectively. The simulations of ODVR for more realistic Earth models were based on implementation of available for different lithology empirical relationships (section 3) with worldwide real case experience in forward modelling of target phenomena and calibration of the relevant basin models. The regions with rather different geology – stratigraphy settings were involved: the North Sea, Petchora Sea, Jeanne D'Ark (the continental margin of eastern Canada), Western Siberia and Gulf of Mexico basins. For some of the regions it was possible also to make comparison at control wells between basin model estimation of overpressure and seismically derived predictions based on surface and VSP seismic data.

The extended analyses of real cases and basin model simulations allow to make the following conclusions:

1. The use of seismic velocity as an sensitive parameter within the range of standard velocity → pore pressure conversion models must be controlled by using forward modelling of ODVR to avoid misleading in interpretation. In particular, the upper transition zone, which separates hydrostatic regime (~1.0 g/cm^3 of EMW) from noticeable over-hydrostatic regime (≥1.35 g/cm^3 of EMW) could be surely detectable in mudrocks[5] from available seismic data within monotonous clastic sections on the condition that 5 % error level for interval rock velocity estimation is achievable. Such condition seems to be quite reachable for an upper part (above 2.5 km) of continuously burying basins mainly built up during Cenozoic epoch. The deeper and older part of the section requires significant extension of the background Earth model to be applicable for velocity → pore pressure conversion.
2. Indeed, a data inversion approach provides the most universal framework for generation of purposely conditioned background Earth model and model constrained processing. The more general background model provides more room for accommodation of *a priori* available knowledge and ensures control of its sensitivity and applicability for prediction purposes at any given geology settings. Thus, the main advantage of such kind model driven approach to target oriented seismic data processing in comparison with conventional stacking velocity analysis seems to be in ability to understand and to control the interpretation and to constrain the results with the quantitative confidence level.
3. It is important, however, to realise that substitution of bijective velocity conversion routine on non-unique by definition data inversion process has pretty negative sides in itself. They are well known (see s/section 5.1) and could be accepted as the only alternative where and when locally valid standard approaches become too

[5] The over-hydrostatic anomaly for sandy rock should be higher ($\xi \geq 1.5$ g/cm^3 of EMW).

uncertain and risky for prediction purposes. In connection with such common for inversion disadvantages as non-uniqueness and instability of solution it is important to get the background model properly attributed and upscaled in advance. The *a priori* well defined constrains over a model parameter space with the reasonably certain starting point inside the relevant subset on it are often a guaranty for quickly converging routine and locally unique solution. The inversion approach to 4-D seismic time-lapse data gives an excellent example of reasonably fast and accurate overpressure prediction based on elastic model parameters (see, for example, *Cole et al.*, 2003). The commonly reported success in this field can be explained by two factors: the inversion of 4-D seismic data in contrast to 3-D ones deals with time increment of specific target parameters (not with its absolute value) on condition that the rest of them are fixed for all time-lapse at some reasonable but unknown values or their variations are negligibly small; the target subsurface object (reservoir) is local. Evidently, the relevant model attribute space for such a local 3-D object can be significantly shrunk and purposely upscaled.

4. One of the attractive directions in reducing of unavoidable negative features of seismic data inversion consists in combining of an empirical rock physics model established for seismic velocity vs. lithology with basing model calibrated for specific regions against multi-well offset data. Since the target of prediction is defined in advance (overpressure in our case) the background velocity model could be upscaled for purposes. The properly upscaled and calibrated basin model could deliver in turn pretty close to purposes start velocity model in the form of low frequency lithology depended on multi trend curves for required elastic parameters. This combination potentially allows to create a rather general and flexibly tuneable background Earth model as a prerequisite of understandable and real time updateable overpressure prediction based on multi source data.

Acknowledgements

The author has the pleasure to thank Eugeny F. Bezmaternyhk ("NIIMORGEOFIZIKA Service", Murmansk, Russia) for assistance in getting access to VSP data and interpretation (the Petchora Sea and Western Siberia basins) as well as for his permanent interest to the problem and valuable discussions, which contribute in getting this paper initiated and finally written. The author is also grateful to Jim Bridges ("Knowledge System Inc.", Houston, USA) and Jay Bruton ("Chevron", Houston, USA) for giving opportunity to compare traditional surface velocity analysis results with basin modelling results aimed for pore pressure evaluation in the Gulf of Mexico and Jeanne D'Ark basins. The author also very much appreciates long term collaboration with Eamonn Doyle ("Knowledge System Inc.", Bergen, Norway) who has helped him in getting definitive pore pressure interpretations for the North Sea basins and Eastern Canadian offshore.

References

Alberty M.W., McLean R.M. Emerging trends in pressure prediction. *OTC 15290 paper presented on "Offshore Technology Conference" held in Houston*, Texas, USA, May 5-8, 2003.

Al-Dajani A.F., Alkhalifah T., Morgan F.D. Reflection moveout inversion in azimutally anisotropic media: Accuracy, limitation and acquisition. *Geophysical Prospecting*, v.47, p.735-756, 1999.

Al-Ghalabi. Seismic velocity – a critique. *The First Break*, v.3, p.36-41, 1994.

Allen P.A., Allen J.R. Basin analysis principles and applications. *Blackwell Scientific Publication, Oxford, London*, 393 p., 1990.

Athy L.R. Compaction and oil migration. *The American Association of Petroleum Geologists Bulletin*, v.14, p.25-36, 1930.

Averbukh A.G. Investigation of sedimentary rock properties and content by using seismic. *Moscow, Nedra*, 232 p., 1982 (in Russian).

Avtchan G.M., Matveenko A.A., Stefankevich Z.B. The petro-physics of sedimentary rocks at great depth conditions. *Moscow, Nedra*, 223 p., 1979 (in Russian).

Bach T., Espersen T.B., Pedersen J., Rasmussen K. Inversion of seismic AVO data. *Lecture Notes in Earth Sciences (Methods and Applications of Inversion)*, v.92, p.31-42, 2000.

Backus G.E. Long way anisotropy produced by horizontal layering. *Journal of Geophysical Research*, v.67, p.4427-4440, 1962.

Baldwin B., Butler C.O. Compaction curves. *The American Association of Petroleum Geologists Bulletin*, v.69, p.622-626, 1985.

Bangs N.L., Moor G.E., Shipley T.H. Elevated fluid pressure and fault zone dilation inferred from seismic models of the North Barbados Ridge decollement. *Journal of Geophysical Research*, v.101, p.627-642, 1996.

Bell S. HPHT wells present safety, cost control challenges. *Journal of Petroleum Engineer International*, June, p.54-55, 1994.

Berryman J.G. Long-wavelength propagation in composite elastic media. Special inclusions. *Journal of Acoustical Society of America*, v.68, p.1809-1819, 1980.

Berryman J.G., Milton G.W. Microgeometry of random composites and porous media. *Applied Physics*, v.21, p.87-94, 1988.

Berryman J.G., Milton G.W. Exact results for generalised Gassmann's equations in composite porous media with two constituents. *Geophysics*, v.56, p.1950-1960, 1991.

Best A. Influence of pressure on ultrasonic velocity and attenuation in near surface sedimentary rock. *Geophysical Prospecting*, v.45, p.345-364, 1997.

Bilgeri D., Ademeno E.B. Predicting abnormally pressured sedimentary rocks. *Geophysical Prospecting*, v.30, p.608-621, 1982.

Biot M.A. Theory of propagation of elastic waves in a fluidsaturated porous solid. Low-frequency range. *Applied Physics*, v.13, p.35-40, 1956.

Bleistein M., Cohen J.K., Stockwell J.W.Jr. Mathematics of multidimensional seismic imaging. Migration and inversion. *Interdisciplinary Applied Mathematics*, v.13, 510 p., 2001.

Botieva T.A., Shoulova N.S. Generation and accumulation of HC reserves within Timan-Petchora oil province. *Sovetskaya Geologiya*, v.9, p.13-19, 1991 (in Russian).

Bowers G.L. Pore pressure estimation from velocity data: Accounting for overpressure mechanisms besides undercompaction. *SPE Drilling and Completion*, v.6, p.89-95, 1995.

Brandt H. A study of the speed of sound in porous granular media. *Journal Applied Mechanics*, v.22, p.479-486, 1955.

Brown R.J.S., Korringa J. On the dependence of the elastic properties of a porous rock on the compressibility of a pore fluid. *Geophysics*, v.40, p.608-616, 1975.

Buhrig C. Geopressured Jurassic reservoirs in the Viking Graben: Modelling and geological significance. *Marine and Petroleum Geology*, v.6, p.35-48, 1989.

Campbell A., Elam S., Lahann R., Patmore S. Pressure prediction from seismic derived velocities. *Paper presented on "Overpressure 2000" workshop, London*, 4-6 April, 2000.

Carcione J.M. Viscoelastic effective theologies for modelling wave propagation in porous media. *Geophysical Prospecting*, v.46, p.249-270, 1998.

Carcione J.M., Helle H.B. Rock physics of geopressure and prediction of abnormal pore fluid pressure using seismic data. *CSEG Recorder*, September, p.8-31, 2002.

Castagna J.P., Backus M.M. Offset-dependent reflectivity theory and practice of AVO analysis. *Investigations in Geophysics*, v.8, 348 p., 1993.

Charara M., Barnes Ch., Tarantola A. Full waveform inversion of seismic data for viscoelastic medium. *Lecture Notes in Earth Sciences (Methods and Applications of Inversion)*, v.92, p.68-81, 2000.

Cheng C.H., Toksoz M.N. Inversion of seismic velocities for the pore aspect ratio spectrum of a rock. *Journal of Geophysical Research*, v.84, p.7533-7543, 1979.

Chiarelli A., Duffaud F. Pressure origin and distribution in Jurassic of Viking basin (United Kingdom – Norway). *The American Association of Petroleum Geologists Bulletin*, v.64, p.1245-1266, 1980.

Christensen N.I., Wang H.T. The influence of pore and confining pressure on dynamic elastic properties of Berea sandstone. *Geophysics*, v.50, p.207-213, 1985.

Cole S., Lumley D., Meadows M. 4-D pressure and saturation inversion of Schiehallon field by rock physics modelling. *Paper A-05 presented on EAGE*, 2003.

DeKok R., Dutta N.C., Khan M., Gelinsky S.G. Deepwater geo-hazard detection using prestack inversion. *71-st Ann. Internal. Mtg., Soc. Expl. Geophys., Extended Abstracts*, p.613-616, 2001.

Dewhurst D., Siggins T., Wu B., Dodds K. The effect of stress state and fluid pressure on the ultrasonic properties of shales. *Paper presented on "Overpressure 2000 workshop"*, London, 4-6 of April, 2000.

Dix C.H. Seismic velocities from surface measurements. *Geophysics*, v.20, p.66-68, 1955.

Dobrynin V.M., Serebryakov V.A. Methods of prediction of abnormally high pore pressure. *Moscow, Nedra*, 232 p., 1978 (in Russian).

Domenico S.N. Effect of brine-gas mixture velocity in an unconsolidated sand reservoir. *Geophysics*, v.41, p.882-894, 1976.

Düppenbecker S.J., Iliffe J.E., Osborne M.J. The role of multi-dimensional basin modelling in integrated pre-drill pressure prediction. *Paper presented on 11th meeting of the Geologic Modelling Society, Galveston*, 5 September, 2002.

Dutta N.C. Deepwater geohazard prediction using prestack inversion of large offset P-wave data and rock model. *The Leading Edge*, February, p.193-198, 2002a.

Dutta N.C. Fluid flow in low permeable porous media. In: B. Doligez, Ed. Migration of hydrocarbons in sedimentary basins. *Editions Technip*, p.567-595, 1987.

Dutta N.C. Geopressure prediction using seismic data: Current status and the road ahead. *Geophysics*, v.67, p.2012-2041, 2002b.

Dutta N.C. Shale compaction and abnormal pore pressures. A model of geopressures in the Gulf Coast Basin. *53rd Ann. Internal. Mtg., Soc. Expl. Geophys., Expanded Abstracts*, p.542-544, 1983.

Dutta N.C., Borland W.H., Leaney S.W., Meehan R., Nutt W.L. Pore pressure ahead of the bit. An integrated approach. *Am. Assn. Drilling Eng. Forum on Pressure Regimes in Sedimentary Basins and Their Prediction*, 1998.

Dutta N.C., Ray A. Subsurface image of geopressured rocks using seismic velocity and acoustic impedance inversion. *58th Annual Meeting Eur. Assoc. Geosci. Eng., Amsterdam, Extended Abstracts*, 1996.

Dvorkin J., Nur A. Dynamic poroelasticity: A unified model with the squirt and Biot mechanisms. *Geophysics*, v.58, p.524-533, 1993.

Eaton B.A. Graphical method predicts pressure worldwide. *World Oil*, v.182, p.51-56, 1972.

Eberhart-Phillips D., Han D.-H., Zoback M.D. Empirical relationships among seismic velocity, effective pressure, porosity and clay content in sandstone. *Geophysics*, v.54, p.82-89, 1989.

Freund D. Ultrasonic compressional and shear velocities in dry clastic rocks as a function of porosity, clay content, and confining pressure. *Geophysical Journal International*, v.108, p.125-135, 1992.

Gangi A.F., Berg R.R. Primary migration by oil generation fracturing in law permeable source rocks. *The American Association of Petroleum Geologists Bulletin*, v.81, p.424-443, 1997.

Garanin V.A. About elastic and attenuation properties of cemented two-phase porous media detectable on ultrasonic frequency band. *Applied Geophysics*, v.60, p.44-52, 1970 (in Russian).

Gardner G.H.F., Gardner L.W., Gregory A.R. Formation velocity and density. The diagnostic basics of stratigraphic traps. *Geophysics*, v.39, p.770-780, 1974.

Gassmann F. Uber die elastizat poroser medien. *Natur. Ges. Zurich, Vierteljahrssch*, B.96, S.1-23, 1951.

Ge H., Jackson M., Vendevile B.C. Kinematics and dynamics of salt tectonics driven by progradation. *The American Association of Petroleum Geologists Bulletin*, v.81, p.388-423, 1997.

Geertsma J. Velocity log interpretation: The effect of rock bulk compressibility. *Soc. Petroleum Engineers AISME Trans*., v.222, p.235-253, 1961.

Gelchinsky B. The common reflecting element (CRE) method (non-uniform asymmetric multifold system). *Exploration Geophysics*, v.19, p.71-75, 1988.

Goffe W.L., Ferrier G.D., Rodgers J. Global optimisation of statistical functions with simulated annealing. *Journal Econometrics*, v.60, p.65-100, 1994.

Goldberg. Genetic algorithms in search optimisation and machine learning. *Addison Wesley Publ. Co*., 1989.

Goldin S.V. Seismic traveltime inversion. *Investigations in Geophysics. Tulsa: OK, USA 1*, 363 p., 1986.

Grant A.C., McAlpine K.D., Wade J.A. The continental margin of eastern Canada – geological framework and petroleum potential. In: Future petroleum provinces of the world. Edited by M.T. Halbouty. *American Association of Petroleum Geologists*, v.40, p.177-205, 1986.

Grechka V., Tsvankin I., Cohen J.K. Generalised Dix equation and analytic treatment of normal-moveout velocity for anisotropic media. *Geophysical Prospecting*, v.47, p.117-148, 1999.

Gregory A.R. Fluid saturation effects on dynamic elastic properties of sedimentary rocks. *Geophysics*, v.41, p.895-921, 1976.

Han D., Nur A., Morgan D. Effects of porosity and clay content on wave velocities in sandstones. *Geophysics*, v.51, p.2093-2107, 1986.

Hattmann C.E., Johnson R.K. Estimation of formation pressures from log-derived shale properties. *Journal Petroleum Technology*, v.17, p.717-722, 1965.

Helth A.E., Walsh J.J., Watterson J. Estimation of effects of sub-seismic sealing faults on effective permeabilities in sandstone reservoirs. *North Sea and Gas Reservoirs*, v.3, p.173-183, 1994.

Hubbert M.K., Rubey W.W. Role of fluid pressures in mechanics of overthrust faulting. *Geological Society of America Bulletin*, v.70, p.115-166, 1959.

Huffman A.R. The future of pore pressure prediction using geophysical methods. *The Leading Edge*, February, p.199-205, 2002.

Introduction to the petroleum geology of the North Sea. Ed. by Glenkie K.W. *Oxford, London*, 236 p., 1984.

Issler D.R. A new approach to shale compaction and stratigraphic restoration: Beaufort-McKenzie basin and McKenzie corridor, North Canada. *The American Association of Petroleum Geologists Bulletin*, v.76, p.1170-1189, 1992.

Karig D.E., Hou G. High stress consolidation and their geological implication. *Journal of Geophysical Research*, v.97, p.289-300, 1992.

Katsube N., Caroll M.M. The role of Terzaghi's effective stress in linearly elastic deformation. *Journal of Energy Resources Technology*, v.105, p.509-511, 1983.

Keller T., Motschmann U., Engelhard L. Modelling the poroelasticity of rocks and ice. *Geophysical Prospecting*, v.47, p.509-526, 1999.

Keyser W., Johnston L.K., Reeves R., Rodriguez G. Pore pressure prediction from surface seismic. *World Oil*, v.9, p.115-122, 1991.

Khaksar A., Griffiths C.M. Influence of effective stress on acoustic velocity and log derived porosity. *SPE Reservoir Evaluation Engineering*, v.2, p.69-74, 1999.

Khaksar A., Griffiths C.M., McCann C. Compressional- and shear-wave velocities as a function of confining stress in dry sandstones. *Geophysical Prospecting*, v.47, p.487-508, 1999.

Khazanehdari J., McCann C., Sothcott J. The effects of pore fluid pressure, confining pressure and pore fluid types on acoustic properties of a suite of clean sandstones. *Paper presented on conference "Pressure Regimes in sedimentary basins and their prediction", Sept. 2-4, DelLago, Texas, USA*, 1998.

King M.S. Wave velocity in rock as a function of changes in overburden pressure and pore fluid saturants. *Geophysics*, v.31, p.50-73, 1966.

King M.S., Marsden J.R., Dennis J.W. Biot dispersion for P- and S-wave velocities in partially and fully saturated sandstones. *Geophysical Prospecting*, v.48, p.1075-1089, 2000.

Kontorovitch A.Eh., Nesterov I.I., Salmanov F.K. Oil and gas geology of Western Siberia. *Moscow, Nedra*, 680 p., 1975 (in Russian).

Kool H. Insufficiency of compaction disequilibrium as a sole cause of high pore fluid pressure in pre-Cenozoic sediments. *Basin Research*, v.9, p.227-241, 1997.

Krouglikov N.M., Nelubin V.V., Yakovlev O.N. Hydro-geology of Western Siberia oilbearing basin in connection with the oil and gas field accumulations. *Leningrad, Nedra*, 279 p., 1985 (in Russian).

Kuster G.T., Toksoz M.N. Velocity and attenuation of seismic waves in two-phase media. Part I. Theoretical formulations. *Geophysics*, v.39, p.587-606, 1974.

Lahann R.V., McCarty D.K., Hsieh J.C.C. Influence of clay diagenesis on shale velocity and fluid pressure. *Paper OTC 13046 presented on "Offshore Technology Conference", Houston*, 30 April – 3 May, 2001.

Landro M. Discrimination between pressure and fluid saturation changes from time laps seismic data. *Geophysics*, v.31, N 1, p.50-73, 2001.

Lerch I. Theoretical aspects of problems in basin modelling. In: "Basin modelling advances and applications". *Norwegian petroleum society (NPF ©). Special publication, Elsevier, Amsterdam*, v.3, p.35-65, 1990.

Littke R., Cramer B., Gerling P., Lopatin N.V., Poelchau H.S, Schaefer R.G., Welte D.H. Gas generation and accumulation in the Western Siberia basin. *AAPG*, v.83, p.1642-1665, 1999.

Lopez J.L., Rappold R.M., Ugueto G.A., Wieseneck J.B., Vu G.K. Integrated shared Earth model: 3-D pore pressure prediction and uncertainty analysis. *The Leading Edge*, January, p.52-59, 2004.

Luo X., Brigaud F., Vasseur G. Compaction coefficients of agrillaceous sediments: Their implications, significance and determination. In: *"Basin Modelling Advances and Applications" Norwegian Petroleum Society (NPF ©), Special publication, Elsevier, Amsterdam*, v.3, p.321-332, 1993.

Luo X., Vasseur G. Contributions of compaction and aquathermal pressuring to geopressure and the influence of environmental conditions. *The American Association of Petroleum Geologists Bulletin*, v.76, p.1550-1559, 1992.

Luo X., Vasseur G. Geopressuring mechanism of organic matter cracking: Numerical modelling. *The American Association of Petroleum Geologists Bulletin*, v.80, p.856-874, 1996.

Madatov A.G., Helle H.B., Sereda V-A.I. Attenuation from inversion of surface seismic data – application to the pore pressure prediction. *Paper presented in SEG'96 summer workshop "Big Sky"*, Montana, 1996a.

Madatov A.G., Helle H.B., Sereda V-A.I. Modelling and inversion technique applied to pore pressure evaluation. *Paper (E048) presented at 57-th EAGE Conference Glasgow*, 29 May – 2 June, 1995.

Madatov A.G., Mitrofanov G.M., Sereda V.-A.I. Approximation approach in dynamic analysis of seismograms. Part 2. Parameter estimation. *Soviet Geology and Geophysics*, v.32, p.101-110, 1991.

Madatov A.G., Sereda A.-V.I. The forward and inverse problems of the fluid dynamics in basin modelling applied to the pore pressure prediction within the sedimentary basins. P.2. The practical aspects. *Proceedings of the Murmansk State Technical University*, v.3, p.351-366, 2000b.

Madatov A.G., Sereda A.-V.I. Upscaling of a basin model required for pore pressure prediction before and during drilling. *Proceedings of the Murmansk State Technical University*, v.6, p.119-144, 2003.

Madatov A.G., Sereda A.-V.I., Doyle E.F., Helle H.B. The "1.5-D" inversion approach to the pore pressure evaluation. Concept and application. *Paper presented on workshop "Compaction and Overpressure Current Research", 9-10 December, Institute Francis du Petrol, Paris, France*, 1996b.

Madatov A.G., Sereda V.-A.I. The forward and inverse problems of the fluid dynamics in basin modelling applied to the pore pressure prediction within the sedimentary basins. P.1. Theory aspects. *Proceedings of the Murmansk State Technical University*, v.3, p.89-114, 2000a.

Madatov A.G., Sereda V.-A.I., Doyle E.F. Integration and inversion of well data into the basin evolution model: Way to the new generation of pressure prediction technologies. *Paper presented on forum "Pressure regimes in sedimentary basins and their prediction" Houston, Texas, USA*, 2-4 September, 1998.

Madatov A.G., Sereda V.-A.I., Doyle E.F. Pore pressure prediction by using inversion before and during drilling. *Paper presented on workshop "New methods and technologies in petroleum geology, drilling and reservoir engineering", Krakow, Poland*, 19-20 June, 1997.

Magara K. Compaction and fluid migration. *Elsevier Scientific Publishing Company*, 319 p., 1978.

Mathew W.R., Kelly J. How to predict formation pressure and fracture gradient. *Oil and Gas J.*, v.65, p.92-106, 1967.

Matlick S. Model-based inversion of amplitude-variation with offset data using a genetic algorithm. *Geophysics*, v.60, p.939-954, 1995.

McAlpine K.D. Mesozoic stratigraphy, sedimentary evolution, and petroleum potential of the Jeanne d'Arc Basin. Grand Banks of Newfoundland. *Geologic Survey of Canada*, paper 8917, 50 p., 1990.

McCann C., Sothcott J. Laboratory measurements of the seismic properties of sedimentary rocks. *Geological Applications of Wirelinc Logs II, Geological Society Special Publication*, v.65, p.285-297, 1992.

Mehta C.H. Scattering theory of wave propagation in a two-phase medium. *Geophysics*, v.48, p.1359-1370, 1983.

Meissner F.F. Examples of abnormal fluid pressure produced by hydrocarbon generation. *Geophysics*, v.46, p.446, 1981.

Mello U.T., Karner G.D. Development of sediment overpressure and its effect on thermal maturation. Application to the Gulf of Mexico basin. *The American Association of Petroleum Geologists Bulletin*, v.80, p.1367-1395, 1996.

Menke W. Geophysical data analysis. Discrete Inverse Theory. *Academic press, New York*, 312 p., 1984.

Mouchet J.P., Mitchell A. Abnormal pressures while drilling. Manuals techniques. *Elf Aquitaine*, *Boussens*, 286 p., 1989.

Mudford B.S. A one-dimensional, two-phase model of overpressure generation in the Venture gas field, offshore Nova Scotia. *Bulletin of Canadian Petroleum Geology*, v.38, p.246-258, 1990.

Mudford B.S. Modelling the occurrence of overpressures on the Scotian shelf. Offshore Eastern Canada. *Journal of Geophysical Research*, v.93, p.7845-7855, 1988.

Nur A., Dvorkin J. Critical porosity: The key factor to relating velocity to porosity in rocks. *Paper presented on conference "Pressure Regimes in sedimentary basins and their prediction", DelLago, Texas, USA*, 2-4 September, 1998.

Nur A.M., Wang Z.Eds. Seismic and acoustic velocities in reservoir rocks. 2. Theoretical and model studies. *Society Exploration Geophysics*, 1992.

Palciauskas V.V., Domenico P.A. Fluid pressures in deforming porous rocks. *Water Resources Research*, v.25, p.203-213, 1989.

Pennebaker E.S. Seismic data indicate depth and magnitude of abnormal pressure. *World Oil*, v.166, p.73-82, 1968.

Pennington W.D., Acevedo H., Green A., Haataja J., Len S., Minaeva A., Xie D. Calibration of seismic attributes for reservoir characterisation. *Final Report MTU, Houghton*, 185 p., 2002 (www.geo.mtu.edu/spot/calibration seismic).

Pickett G.R. Acoustic character logs and their application in formation evaluation. *J. Petr. Tech*., v.15, p.659-667, 1963.

Prasad M., Manghnani M.H. Effects of pore and differential pressure on compressional wave velocity and quality factor in Berea and Michigan sandstones. *Geophysics*, v.62, p.1163-1176, 1997.

Raiga-Clemenceau J., Martin J.P., Nicoletis S. The concept of acoustic formation factor for more accurate porosity determination from sonic transit time data. *The Log Analyst*, v.29, p.54-60, 1988.

Reike H.H., Chilingarian G.V. Compaction of argillacious sediments. *London, New York*, 424 p., 1974.

Reynolds E.B. Predicting overpressured zones with seismic data. *World Oil*, v.171, p.78-82, 1970.

Rowan M.G. A systematic technique for the sequential of salt structures. *Tectonophysics*, v.228, p.369-381, 1993.

Sayers C.M., Johnston J.M. Pre-drill pore pressure prediction using seismic data. *Paper presented on "Overpressure 2000" workshop, London*, 4-6 April, 2000.

Sayers C.M., Woodward M.J., Bartman R.C. Seismic pore pressure prediction using reflection tomography and 4-C seismic data. *The Leading Edge*, February, p.188-192, 2002.

Schneider F., Potdevin J.L., Wolf S., Faille L. Model de compaction elastoplastique et viscoplastique pour simulator de basins sedimentaires. *IPF Revue*, v.49, p.141-148, 1994.

Seberyakov V.A., Chilingarian G.V., Katz S.A. Methods of estimating and predicting abnormal formation pressure. *Journal of Petroleum Science and Engineering*, v.13, p.113-123, 1995.

Sejourne C., Beaufort D., Brunel C. What is the impact of shale anisotropy on pore pressure prediction before drilling? *Paper presented on "Overpressure 2000" workshop, London*, 4-6 April, 2000.

Smith J.E. The dynamics of shale compaction and evaluation of pore-fluid pressure. *Mathematics Geology*, v.3, p.239-263, 1971.

Solomatin A.V. The oil and gas prospects in late Devonian section of Varanday-Adzvinsokaja zone of Timan-Petchora oil province. *Geologiya nefti i gaza*, v.10, p.23-25, 1988 (in Russian).

Swarbrick R.E., Osborne M.J. The nature and diversity of pressure transition zones. *Petroleum Geoscience*, v.2, p.111-116, 1996.

Tao G., King M.S., Nabi-Bidhendi M. Ultrasonic wave propagation in dry and brine-saturated sandstones as a function of effective stress: Laboratory measurements and modelling. *Geophysical Prospecting*, v.43, p.299-327, 1995.

Tarantola A. Inverse problem theory: Methods for data fitting and model parameter estimation. *Elsevier*, *Netherlands*, 386 p., 1987.

Tarantola A. Inversion of seismic reflection data in the acoustic approximation. *Geophysics*, v.49, p.1259-1266, 1984.

Terzaghi K., Peck R.B. Soil mechanics in engineering practice. *Wiley, New York*, 566 p., 1948.

Tikhonov A.N., Arsenin V.Ja. The methods of solution of ill-posed problems. *Moscow, Nauka*, 285 p., 1979 (in Russian).

Tissot B.P., Welte D.H. Petroleum formation and occurrence. *Springer-Verlag, New York*, 538 p., 1978.

Toksoz M.N., Cheng C.H., Timur A. Velocities of seismic waves in porous rocks. *Geophysics*, v.41, p.621-645, 1976.

Tosaya C.A. Acoustical properties of clay-bearing rocks. *Published Ph.D. Thesis, Stanford University, USA*, 136 p., 1982.

Traugott M.O. Pore-fracture pressure determinations in deep water. *World Oil, Deepwater Technology supplement*, August, 1997.

Traugott M.O. The pore pressure centroid concept. Reducing Drilling Risk – Compaction and Overpressure Current Research. *Abst., IFP, Paris*, 9-10 December, 1996.

Traugott M.O. Use of model-derived compaction trend lines in pore pressure prediction methods. *Paper presented on "Overpressure 2000" workshop, 4-6 April, London*, 2000.

Urupov A.K., Levin A.N. Detecting and interpretation of seismic velocities in reflection waves' method. *Moscow, Nedra*, 288 p., 1985 (in Russian).

Vernik L. Predicting lithology and transport properties from acoustic velocities based on petrophysical classification of siliclastics. *Geophysics*, v.59, p.420-427, 1994.

Vernik L. Predicting porosity from acoustic velocity in siliclastics: A new look. *Geophysics*, v.62, p.118-128, 1997.

Vernik L., Landis C. Elastic anisotropy of source rocks: Implications for hydrocarbon generation and primary migration. *The American Association of Petroleum Geologists Bulletin*, v.80, p.531-544, 1996.

Waples D.W., Kamata H. Modelling porosity reduction as a series of chemical and physical processes. *NPF Elsevier, Amsterdam, Special Publication*, v.3, p.303-320, 1993.

White J.E. Underground sound. *Elsevier, Amsterdam – Oxford – New York*, 264 p., 1983.

Wyllie M.R. An experimental investigation of factors affecting elastic wave velocities in porous media. *Geophysics*, v.23, p.459-493, 1957.

Wyllie M.R.J., Gregory A.R., Gardner G.H.F. An experimental investigation of factors, affecting elastic wave velocities in porous media. *Geophysics*, v.28, p.459-493, 1958.

Wyllie M.R.J., Gregory A.R., Gardner L.W. Elastic wave velocities in heterogeneous and porous media. *Geophysics*, v.21, p.41-70, 1956.

Yassir N.A., Bell J.S. Relationships between pore pressure, stress and present day geodynamics in the Scotian shelf. Offshore Eastern Canada. *The American Association of Petroleum Geologists Bulletin*, v.78, p.1863-1880, 1994.

Yin C.S., Batzle M.L., Smith B.J. Effect of partial liquid/gas saturation on extensional wave attenuation in Berea sandstone. *Geophysical Research Letters*, v.19, p.1399-1402, 1992.

Yu G., Vosoffand K., Durney D.W. Effect of pore pressure on compressional wave velocity in coals. *Exploration Geophysics*, v.22, p.475-480, 1991.

Zagoulova O.P., Yeseptchuk E.D., Larskaya E.S. Influence of plate tectonics development of Timan-Petchora oil province on establishment of source rock formations. *Sovetskaya Geologiya*, v.3, p.10-16, 1994 (in Russian).

Zimmer M., Prasad M., Mavko G. Pressure and porosity influences on Vp-Vs ratio in unconsolidated sands. *The Leading Edge*, February, p.178-183, 2002.

APPENDIX

Notifications:

ρ_0 and ρ_1	density of solid and pore fluid parts of rock
ϕ	porosity
z	depth
H and K	rock matrix compaction constants in vertical stress and depth normal compaction trends, respectively
G	geopressure
σ	vertical (Effective) stress
$H(z) = \rho_1 g z$	hydrostatic pressure
$P(\phi) = G - \sigma(\phi)$	pore pressure in one-axial Terzaghi's approximation

The current porosity according to porosity vs. effective stress normal compaction trend is given by (*Hubbert, Rubey*, 1959; *Palciauskas, Domenico*, 1989):

$$\phi(\sigma_N) = \phi_0 \exp(-K\sigma_N), \quad (1)$$

where σ_N denotes the effective stress on condition of normally compacted by vertical load sediments. Let us use term *Normal Stress*, referring to such conditions. Evidently, for homogeneous lithology with no mineral density changes it can be represented as a function of current porosity ϕ by the following formula:

$$\sigma_N = (\rho_0 - \rho_1)(1 - \phi)gz. \quad (2)$$

The current porosity according to porosity vs. depth normal compaction trend for the same section is given by (*Athy*, 1930):

$$\phi(z) = \phi_0 \exp(-Hz). \quad (3)$$

From (1), (2) and (3) one can get

$$K = H[(\rho_0 - \rho_1)(1 - \phi)g]^{-1}. \quad (4)$$

Let K_N, H_N in agreement with (1) and (3) be compaction coefficients calibrated for sediments, which were not affected by any additional to σ_N components of acting stress (it could be true, for example, in surely tectonically relaxed area located faraway from salt dome influence). Let K, H, respectively, be compaction coefficients calibrated for sediments at any point of calibration area (for example, in proximity to salt dome influence).

Let the measure of abnormal rock compaction be defined as the following:

$$\gamma = (K - K_N) / K_N = (H - H_N) / H_N. \quad (5)$$

Additional vertical component to the *Normal Stress* induced by the salt body seaward rising σ_S can be derived from condition of equal impact on porosity reducing from expressions (1) and (3). Namely, from $K\sigma_N = K_N(\sigma_N + \sigma_S)$ one can get

$$\sigma = [(K - K_N) / K_N]\,\sigma_N = \gamma\sigma_N. \quad (6)$$

Now the abnormal rock compaction constant can be interpreted as a portion of Normal Stress contributing from additional stress sources apart from vertical load during sediment burial (for example, from salt uprising diapir within the local compression areas).